New Insights into the Bromination Reaction for a Series of Alkenes—A Computational Study

Shahidul M. Islam and Raymond A. Poirier*

Department of Chemistry, Memorial University, St. John's, Newfoundland A1B 3X7, Canada

Received: July 19, 2007; In Final Form: September 11, 2007

Ab initio calculations were carried out for the reaction of Br_2 with ethene, propene, isobutene, fluoroethene, chloroethene, (*E*)-1,2-difluoroethene, and (*E*)-1,2-dichloroethene. For ethene the calculations were also carried out for the reaction with $2Br_2$. Geometries were optimized at the HF, MP2, and B3LYP levels using the 6-31G(d) and 6-31+G(d) basis sets where for Br both the standard 6-31G and the Binning−Curtiss bromine basis sets were used. Energies were also calculated at the G3MP2 and G3MP2B3 levels. For a single Br_2 one mechanism involves a perpendicular attack by Br_2 to the C=C bond, and a second mechanism consists of sidewise attack by Br_2. Alkenes can react with $2Br_2$ via several mechanisms, all leading to the dibromo product. The most likely pathway for the reaction of ethene and $2Br_2$ involves a trans addition of a Br atom from Br_3^- to one of the bromonium ion carbons. Activation energies, free energies, and enthalpies of activation along with thermodynamic properties (ΔE, ΔH, and ΔG) for each reaction were calculated. We have found that the reaction of ethene with $2Br_2$ is favored over reaction with only Br_2. There is excellent agreement between the calculated free energies of activation for the reaction of ethene and $2Br_2$ and experimental values in nonpolar aprotic solvents. However, the free energies of activation for the reaction with a single Br_2 agrees well with the experimental results for polar protic solvents only when the reaction is mediated by a solvent molecule. A kinetic expression is proposed that accounts for the difference between bromination of alkenes in protic and nonprotic solvents. Some previously unknown heats of formation are reported.

1. Introduction

The electrophilic addition of Br_2 to alkenes is a well-known organic reaction.[1,2] The reaction mechanism has been extensively studied experimentally, and the generally accepted reaction scheme consists of several steps.[2−7] Studies of this reaction go back to as early as 1937 from the work of Roberts and Kimball.[8] Their work suggested the existence of a cyclic bromonium ion intermediate, which was shown in the late 1960s using NMR, by Olah and co-workers,[9,10] to be the actual reactive species. However, there was no structural evidence for the existence of a cyclic bromonium ion because the reaction is too fast. There have been many experimental attempts by a variety of techniques to confirm the occurrence of cyclic bromonium ions in the gas phase, including photoionization,[11] ion cyclotron resonance,[11−14] radiolytic technique,[15] and conventional mass spectrometry.[16,17] Although some experiments suggest the formation of a bromonium ion, no conclusive evidence could be provided for its actual structure. Strating et al.[18] first produced a bromonium ion tribromide in the lab by reacting adamantylideneadamantane (Ad=Ad) with Br_2 in CCl_4. Slebocka-Tilk et al.[19] for the first time obtained the X-ray structure of adamantylideneadamantane bromonium ion with a Br_3^- counterion. In this case, because back-side attack by Br^- is sterically hindered, bromination stops at the adamantylideneadamantane bromonium ion. (*E*)-2,2,5,5-Tetramethyl-3,4-diphenylhex-3-ene is the first reported example of an olefin whose interaction with bromine is limited to π complex formation.[20] Similarly, tetraneopentylethylene does not react with bromine in CCl_4, and on the basis of the ^{13}C NMR spectrum there is no evidence of formation of a π complex.[21] Thus the reactivity of olefins toward bromine depends on their steric hindrance. A study of the product of bromination of ethene in dichloroethane by ^1H and ^2H NMR spectra indicates that the addition gives *trans*-1,2-dibromoethane.[22] Chretien et al.[23] studied the selectivity of alkene bromination by using stereo-, regio-, and chemoselectivity. It is believed that the electrophilic bromination of alkenes follows a mechanism that has three successive steps: (i) fast-equilibrated formation of an olefin−bromine charge-transfer complex, (ii) rate-limiting ionization of this π complex into a σ complex, the so-called bromonium ion, and, finally, (iii) fast product formation by nucleophilic trapping of the ionic intermediate.[24−26]

In comparison to experimental studies, there have been a limited number of theoretical studies on the bromination of alkenes. Yamabe et al.[27] studied the electrophilic addition reactions $X_2 + C_2H_4 \rightarrow C_2H_4X_2$ (X = F, Cl, and Br) at the MP3/3-21G//RHF/3-21G level of theory. Their study shows that the fluorination of ethene occurs via a four-center transition state, while chlorination and bromination give zwitterionic three-center transition states. The activation energies were found to be 212.5, 212.1, and 256.9 kJ mol^{-1} for X = F, Cl, and Br, respectively. Hamilton and Schaefer[28] in their study on the structure and energetics of $C_2H_4Br^+$ isomers proposed that the transition state for the bromination reaction is a three-membered bromonium ion with a nearby counter bromide ion. Later, Cammi et al.[29] conducted a detailed MP2 study from the charge-transfer complex (CTC) to the transition state (TS) for the addition of Br_2 to ethene both in the gas phase and in water. At the MP2/CEP-121G(aug) level the structures of the CTC and the TS were found to have C_{2v} symmetry both in the gas phase and in water. They also found that the structure of the CTC is not very

* Author to whom correspondence should be addressed. Phone: (709) 737-8609. Fax: (709) 737-3702. E-mail: rpoirier@mun.ca.

10.1021/jp075674b CCC: $37.00
Published on Web 11/15/2007

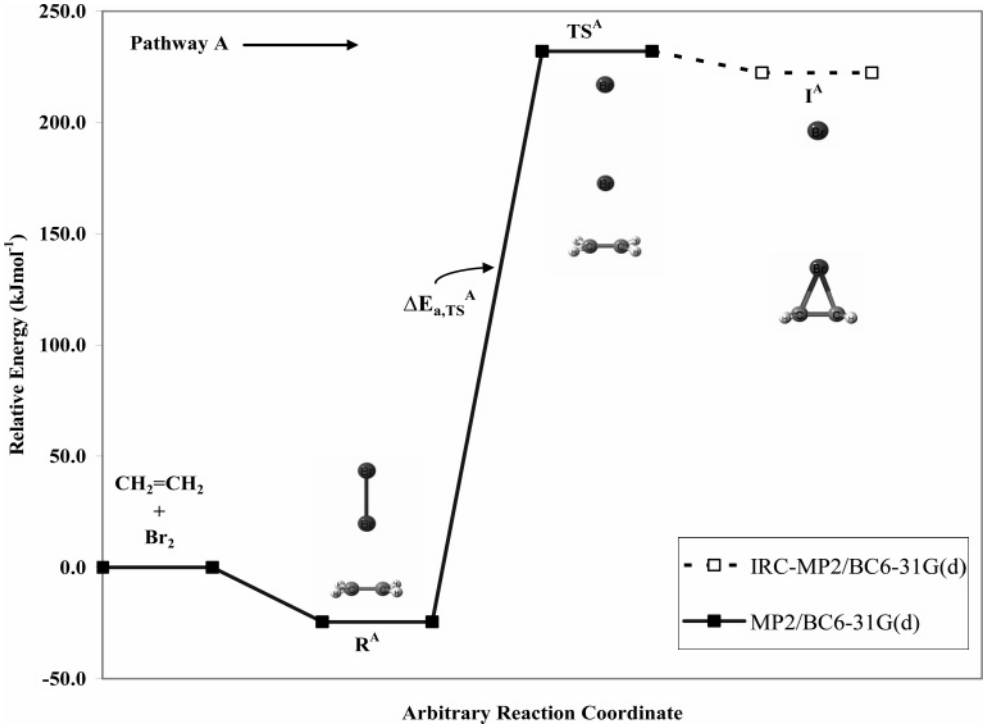

Figure 1. Pathway and barrier for the reaction of $CH_2{=}CH_2 + Br_2$ (pathway A) at the MP2/BC6-31G(d) level of theory. Although the IRC leads to I^A, no optimized structure was found.

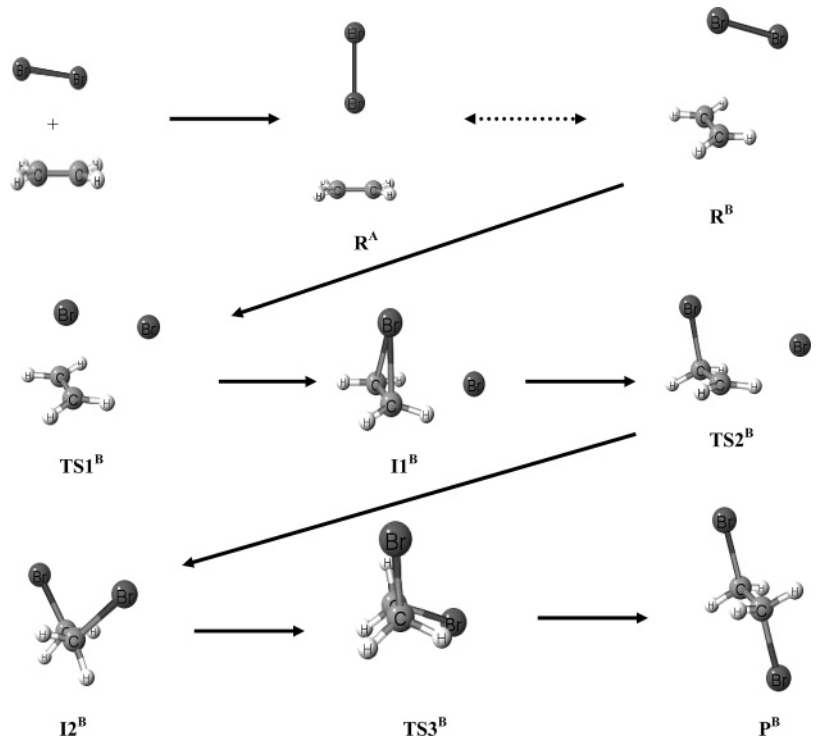

Figure 2. Mechanism for the reaction of $CH_2{=}CH_2 + Br_2$ (pathway B). Similar structures are found for the bromination of $CH_3{-}CH_2{=}CH_2$, $(CH_3)_2CH{=}CH_2$, $CH_2{=}CHF$, and $CH_2{=}CHCl$.

different in the gas phase and in water, but the TS structure is largely affected by the presence of the solvent where the solvated TS has an earlier character with a Br−Br bond much shorter than that in the gas phase. At the MP2/CEP-121G(aug) level the barrier was found to be 250.8 kJ mol^{-1}. The first step in electrophilic bromination of ethene in water was also investigated by Strnad et al.[30] by molecular dynamics simulations. Hamilton and Schaefer[28,31] studied the structure and energetics of $C_2H_4Br^+$, $C_2H_2Br^+$, and $C_2H_2Cl^+$ using ab initio quantum mechanical techniques and found that the cyclic bromonium ion is more stable than the acyclic 1-bromoethyl cation by 6.3 kJ mol^{-1} with a barrier of 104.5 kJ mol^{-1} for the interconversion of these two forms. Cossi et al.[32] found the positive charge to be delocalized over the Br atom and the two olefinic carbons in the bromonium ion. The CTC formed during the first step of the bromination reaction was also investigated.[33−35]

TABLE 1: Activation Energies, Free Energies, and Enthalpies of Activation (kJ mol^{-1}) at 298.15 K for the Reaction of CH_2=CH_2, CH_3−CH_2=CH_2, $(CH_3)_2CH$=CH_2, CH_2=CHF, CH_2=CHCl, (*E*)-CHF=CHF, and (*E*)-CHCl=CHCl with Br_2 (Pathway A)[a,b]

level/basis set	$\Delta E_{a,TS}^{A}$	$\Delta G^{\ddagger}_{TS}{}^{A}$	$\Delta H^{\ddagger}_{TS}{}^{A}$
		CH_2=CH_2 + Br_2	
MP2/6-31G(d)	238.4	229.8	235.2
MP2/BC6-31G(d)	256.4	251.7	250.6
MP2/6-31+G(d)	238.3	231.7	235.2
MP2(FULL)/6-31G(d)	240.9	231.1	237.6
MP2/G3MP2large //MP2(FULL)/6-31G(d)	268.5		
		CH_3−CH_2=CH_2 + Br_2	
MP2/6-31G(d)	230.6	219.6	227.2
MP2/BC6-31G(d)	249.8	236.6	246.3
MP2(FULL)/6-31G(d)	233.5	221.8	230.1
MP2/G3MP2large //MP2(FULL)/6-31G(d)	262.6		
		$(CH_3)_2C$=CH_2 + Br_2	
MP2/6-31G(d)	224.1	211.7	220.7
MP2/BC6-31G(d)	244.8	230.7	241.1
MP2(FULL)/6-31G(d)	227.6	214.4	224.0
MP2/G3MP2large //MP2(FULL)/6-31G(d)	258.2		
		CHF=CH_2 + Br_2	
MP2/6-31G(d)	230.2	224.7	227.6
MP2/BC6-31G(d)	247.6	241.3	244.8
MP2(FULL)/6-31G(d)	232.4	226.3	229.8
MP2/G3MP2large //MP2(FULL)/6-31G(d)	259.6		
		CHCl=CH_2 + Br_2	
MP2/6-31G(d)	228.2	223.5	225.7
MP2/BC6-31G(d)	244.9	238.7	242.1
MP2(FULL)/6-31G(d)	230.4	224.9	227.9
MP2/G3MP2large //MP2(FULL)/6-31G(d)	255.9		
		(*E*)-CHF=CHF + Br_2	
MP2/6-31G(d)	226.1	222.2	223.2
MP2/BC6-31G(d)	243.3	231.4	242.8
MP2(FULL)/6-31G(d)	228.0	222.9	225.1
MP2/G3MP2large //MP2(FULL)/6-31G(d)	254.9		
		(*E*)-CHCl=CHCl + Br_2	
MP2/6-31G(d)	232.6	226.5	229.4
MP2/BC6-31G(d)	249.3	241.2	246.0
MP2(FULL)/6-31G(d)	234.4	226.5	231.2
MP2/G3MP2large //MP2(FULL)/6-31G(d)	256.1		

[a] Barrier as defined in Figure 1. [b] The products are all in a trans conformation.

It is difficult to extract conclusive information about the mechanistic pathways from experiments only. Thus, quantum chemical calculations are the only source for a detailed characterization of the potential energy surface along the reaction path. However, no computational studies have been reported for the complete potential energy surface for the bromination of alkenes. To ensure the reliability of our results, wavefunction and density functional theory (DFT) calculations were performed. Because of the size of the system, it is possible to also perform some calculations at high levels of theory, such as G3MP2 and G3MP2B3, which are known to give reliable energetics.[36,37]

2. Method

All of the electronic structure calculations were carried out with Gaussian 03.[38] The geometries of all reactants, transition states, intermediates, and products were fully optimized at the HF, MP2, and B3LYP levels of theory. From previous work,[39] it was found that for some reactions involving third row elements energetics obtained using the standard 6-31G bromine basis set[40] showed better agreement with G3 theories compared to the Binning−Curtiss[41] bromine (BC6-31G) basis set. Therefore, both the standard 6-31G(d) and BC6-31G(d) bromine basis sets are used in this study. Because the reaction of Br_2 with alkenes is known to proceed through formation of charged species the standard 6-31+G(d) and BC6−31+G(d) basis sets were also used. B3P86 and B3PW91 density functional calculations were also performed where B3LYP failed to give an optimized structure along a reaction pathway. Single-point energies required for G3MP2, G2MP2B3, and G3MP2B3(BC) levels were obtained using the MP2(FULL)/6-31G(d), B3LYP/6-31G(d), and B3LYP/BC6-31G(d) optimized geometries, respectively. For Br, the G3MP2large basis set,[42,43] which is not yet incorporated in Gaussian 03, was used for G3MP2 and G3MP2B3 calculations. Frequencies were calculated for all structures to ensure the absence of imaginary frequencies in the minima and for the presence of only one imaginary frequency in the transition states. The complete reaction pathways for all the mechanisms discussed in this paper have been verified using intrinsic reaction coordinate (IRC) analysis. Structures obtained from IRC have been optimized to positively identify the reactant and product to which each transition state is connected. Free energies of activation and of reaction for the addition reaction of bromine to alkenes in CCl_4, CH_2Cl_2, CH_2Cl−CH_2Cl, and CH_3OH were calculated with the polarizable continuum model (PCM) as implemented in Gaussian 03. All free energy calculations involving solvation were performed using the optimized solution-phase structures. By default, the PCM model builds up the cavity using the united atom (UA0) model, i.e., putting a sphere around each solute heavy atom; hydrogen atoms are enclosed in the sphere of the atom to which they are bonded.

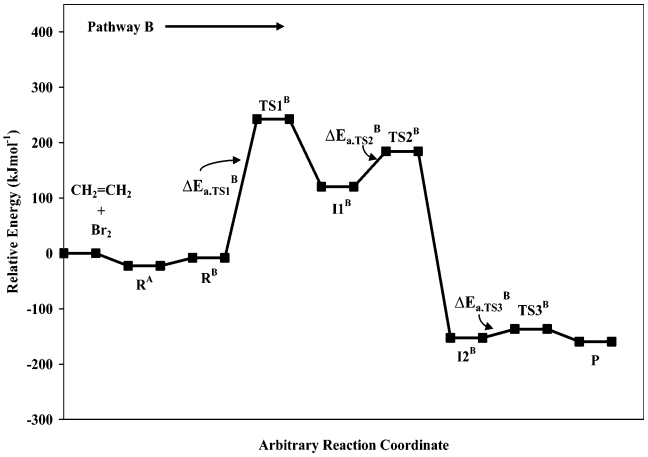

Figure 3. Pathway for the reaction of CH_2=CH_2 + Br_2 (pathway B) at the MP2/BC6-31G(d) level of theory (see Figure 2 for structures).

3. Results and Discussion

The results for the reaction of alkenes with Br_2 and $2Br_2$ are given in Tables 1−9, and the heats of formation of some energetically stable compounds are presented in Table 10.

3.1. Potential Energy Surfaces for the Reaction of Alkenes with Br_2. The results for the reaction of alkenes and Br_2 will be discussed in the following order: (1) perpendicular attack of Br_2 to C=C (pathway A) and (2) sidewise attack of Br_2 to C=C (pathway B).

TABLE 2: Activation Energies, Free Energies, and Enthalpies of Activation (kJ mol^{-1}) at 298.15 K for the Reaction of $CH_2{=}CH_2$, $CH_3{-}CH_2{=}CH_2$, $(CH_3)_2CH{=}CH_2$, $CH_2{=}CHF$, and $CH_2{=}CHCl$ with Br_2 (Pathway B)[a,b,d]

level/basis set		$\Delta E_{a,TS1}{}^B$	$\Delta G^{\ddagger}_{TS1}{}^B$	$\Delta H^{\ddagger}_{TS1}{}^B$	$\Delta E_{a,TS2}{}^B$	$\Delta G^{\ddagger}_{TS2}{}^B$	$\Delta H^{\ddagger}_{TS2}{}^B$	$\Delta E_{a,TS3}{}^B$	$\Delta G^{\ddagger}_{TS3}{}^B$	$\Delta H^{\ddagger}_{TS3}{}^B$
$CH_2{=}CH_2 + Br_2 \rightarrow CH_2Br{-}CH_2Br$										
HF/6-31G(d)		303.0	335.3	301.5	42.7	38.6	37.4	11.4	15.5	9.5
HF/BC6-31G(d)		300.3	320.9	298.5	44.5	40.4	39.4	14.7	16.8	12.6
MP2/6-31G(d)		252.9	275.9	251.0	60.8	57.1	56.5	15.0	15.2	12.7
	CCl_4[e]		262.9			55.8			16.4	
MP2/BC6-31G(d)		247.3	263.5	245.1	58.3	54.8	54.2	18.3	20.0	16.1
B3LYP/6-31G(d)		186.7	212.9	184.7	(36.9)	(33.2)	(37.2)	10.7	11.2	8.5
	CCl_4[e]		191.0			(67.6)			12.3	
B3LYP/BC6-31G(d)		189.1	206.1	186.4	12.3[f]	10.3[f]	9.2[f]	14.0	14.2	11.7
					(9.1)	(8.7)	(6.2)			
B3LYP/6-31+G(d)		193.7	225.7	191.8	(40.8)	(46.4)	(38.4)	10.8	11.2	8.5
B3LYP/BC6−31+G(d)		188.0	208.2	183.3	(14.2)	(13.5)	(11.2)	15.7	15.9	13.2
B3P86/BC6-31G(d)		188.5	199.1	185.9	21.7	18.5	18.4	15.6	15.7	13.3
B3PW91/6-31G(d)		195.1	220.5	195.5	(52.5)	(52.8)	(50.1)	11.6	12.1	9.4
B3PW91/BC6-31G(d)		193.5	214.4	190.7	21.4	18.0	18.1	15.1	15.2	12.9
MP2/G3MP2large//MP2(FULL)/6-31G(d)		250.6	279.0	244.8	63.5	64.1	62.7	16.0	20.5	14.1
MP2/G3MP2large//B3LYP/6-31G(d)		262.0	285.2	256.9	*c*	*c*	*c*	15.6	16.6	13.8
G3MP2		*c*	*c*	*c*	*c*	*c*	*c*	14.4	18.9	12.6
G3MP2B3		*c*	*c*	*c*	*c*	*c*	*c*	13.9	14.9	12.1
$CH_3{-}CH_2{=}CH_2 + Br_2 \rightarrow CH_3{-}CH_2Br{-}CH_2Br$										
HF/6-31G(d)		286.7	317.4	284.5	(17.7)	(13.5)	(12.7)	20.8	23.8	19.0
HF/BC6-31G(d)		283.3	302.2	280.8	22.3	18.5	17.3	23.3	26.1	21.5
MP2/6-31G(d)		201.1	213.2	193.4	45.7	38.8	40.2	23.6	26.3	21.7
	CCl_4[e]		233.5			42.6			26.6	
MP2/BC6-31G(d)		200.4	204.0	190.3	45.0	40.4	39.9	26.8	29.1	24.8
B3LYP/6-31G(d)		167.2	188.5	164.4	(−1.7)	(−3.2)	(−8.6)	17.9	20.9	16.0
B3LYP/BC6-31G(d)		168.1	176.3	167.5	(0.1)	(−1.5)	(−3.8)	20.6	23.1	18.6
	CCl_4[e]		165.9			(42.7)			21.6	
B3LYP/6-31+G(d)		173.4	203.4	170.8	(0.6)	(−0.9)	(−6.8)	18.1	21.2	16.2
B3LYP/BC6−31+G(d)		163.7	177.3	160.7	(8.8)	(6.1)	(4.8)	23.2	26.2	21.3
B3P86/6-31G(d)		167.1	191.3	164.1	*c*	*c*	*c*	19.0	21.9	17.1
B3P86/BC6-31G(d)		166.3	175.9	162.6	13.6	10.3	10.0	22.1	24.5	20.1
B3PW91/6-31G(d)		174.8	205.1	171.8	(6.1)	(0.0)	(4.7)	18.7	21.7	16.9
B3PW91/BC6-31G(d)		170.9	176.4	170.0	13.3	11.0	9.8	21.8	24.3	19.8
MP2/G3MP2large//MP2(FULL)/6-31G(d)		230.7	252.6	228.7	48.9	43.3	48.6	23.9	26.0	23.1
MP2/G3MP2large//B3LYP/6-31G(d)		243.1	263.5	239.3	*c*	*c*	*c*	23.6	26.6	21.5
G3MP2		*c*	*c*	*c*	37.0	31.4	36.7	22.4	24.5	21.6
G3MP2B3		*c*	*c*	*c*	*c*	*c*	*c*	22.0	25.1	20.0
$(CH_3)_2C{=}CH_2 + Br_2 \rightarrow (CH_3)_2CBr{-}CH_2Br$										
HF/BC6-31G(d)		276.2	289.0	272.3	56.1	58.1	52.2	24.6	27.6	22.7
MP2/BC6-31G(d)		189.3	189.7	178.4	54.2	53.0	50.6	28.3	30.8	26.1
B3LYP/BC6-31G(d)		150.7	158.8	145.4	(21.2)	(24.1)	(18.8)	21.3	24.5	19.3
B3LYP/BC6−31+G(d)		146.6	155.0	142.3	(21.3)	(24.3)	(18.8)	24.6	27.6	22.5
B3P86/BC6-31G(d)		147.2	155.1	141.6	(27.4)	(29.4)	(24.9)	23.1	26.2	21.1
B3PW91/BC6-31G(d)		152.2	161.5	146.7	(27.7)	(30.1)	(25.2)	22.9	26.0	20.8
MP2/G3MP2large//B3LYP/BC6-31G(d)		203.3	214.1	200.7	*c*	*c*	*c*	25.2	28.2	22.9
G3MP2B3(BC)		187.4	198.3	184.8	*c*	*c*	*c*	23.3	26.2	21.0
$CHF{=}CH_2 + Br_2 \rightarrow CHFBr{-}CH_2Br$ (Syn Addition of Br_2)										
HF/BC6-31G(d)		327.0	340.5	324.8	13.5	18.4	13.1	15.0	17.3	12.7
MP2/BC6-31G(d)		224.2	234.5	222.4	33.6	37.2	33.4	18.3	20.2	15.8
B3LYP/BC6-31G(d)		190.3	202.5	187.9	7.2	4.9	2.8	13.4	15.5	10.8
B3P86/BC6-31G(d)		187.7	199.5	185.2	6.8	3.4	2.1	15.1	17.2	12.6
B3PW91/BC6-31G(d)		191.6	206.3	189.2	6.4	2.9	1.8	14.6	16.7	12.1
MP2/G3MP2large//B3LYP/BC6-31G(d)		263.8	275.9	260.3	*c*	*c*	*c*	15.7	17.0	13.6
G3MP2B3(BC)		255.6	267.7	252.1	*c*	*c*	*c*	13.8	15.0	11.7
$CHF{=}CH_2 + Br_2 \rightarrow CHFBr{-}CH_2Br$ (Anti Addition of Br_2)										
HF/BC6-31G(d)		299.7	319.7	297.3	(5.1)	(3.6)	(1.8)	25.0	27.4	23.0
MP2/BC6-31G(d)		238.4	253.4	235.8	23.0	20.5	19.5	27.8	29.8	25.5
B3LYP/BC6-31G(d)		177.8	193.2	175.3	(−10.8)	(−13.8)	(−10.7)	29.6	32.4	27.0
MP2/G3MP2large//MP2(FULL)/BC6-31G(d)		250.6	279.0	244.8	63.5	64.1	62.7	16.0	20.5	14.4
MP2/G3MP2large//B3LYP/BC6-31G(d)		259.6	273.8	255.9	*c*	*c*	*c*	25.3	28.1	23.3
G3MP2B3(BC)		252.1	266.3	248.4	*c*	*c*	*c*	23.3	26.1	21.4
$CHCl{=}CH_2 + Br_2 \rightarrow CHClBr{-}CH_2Br$ (Syn Addition of Br_2)										
HF/BC6-31G(d)		330.8	353.8	328.0	16.4	18.0	15.0	19.3	21.8	17.1
MP2/BC6-31G(d)		206.1	221.4	205.0	6.8	10.7	6.1	22.9	25.0	20.5
B3LYP/BC6-31G(d)		191.6	206.9	188.8	25.1	23.9	17.9	18.1	20.3	15.6
MP2/G3MP2large//B3LYP/BC6-31G(d)		236.5	251.2	233.0	60.3	64.3	58.3	19.8	22.5	17.7
G3MP2B3(BC)		217.6	232.3	214.2	34.1	38.1	32.1	17.7	20.4	15.6
$CHCl{=}CH_2 + Br_2 \rightarrow CHClBr{-}CH_2Br$ (Anti Addition of Br_2)										
HF/BC6-31G(d)		309.6	329.9	307.1	(9.7)	(6.8)	(5.7)	32.3	34.4	30.2
MP2/BC6-31G(d)		240.1	255.6	237.4	27.2	23.6	23.2	34.2	36.0	31.9
B3LYP/BC6-31G(d)		180.7	195.9	178.0	(−10.9)	(−14.7)	(−11.0)	27.7	30.0	25.5
MP2/G3MP2large//MP2 (FULL)/BC6-31G(d)		238.1	266.5	232.3	28.5	29.1	27.7	30.2	34.7	28.4
MP2/G3MP2large//B3LYP/BC6-31G(d)		259.0	273.4	255.7	*c*	*c*	*c*	30.6	33.3	28.7
G3MP2B3(BC)		*c*	*c*	*c*	*c*	*c*	*c*	28.3	31.0	26.4

[a] Barriers as defined in Figures 2 and 3, respectively. [b] The values in parentheses are single-point values using optimized MP2 structures. [c] Indicates missing values due to failure to optimize the bromonium/Br^- ion pair or in the QCISD(T) calculation for G3 theories. [d] The products are all in a trans conformation. [e] The PCM-UA0 model was used for optimized structures. In all cases $\Delta G = \Delta\Delta G$ (thermal correction) + ΔG_{solv}. [f] Using MaxStep = 1 for the optimization.

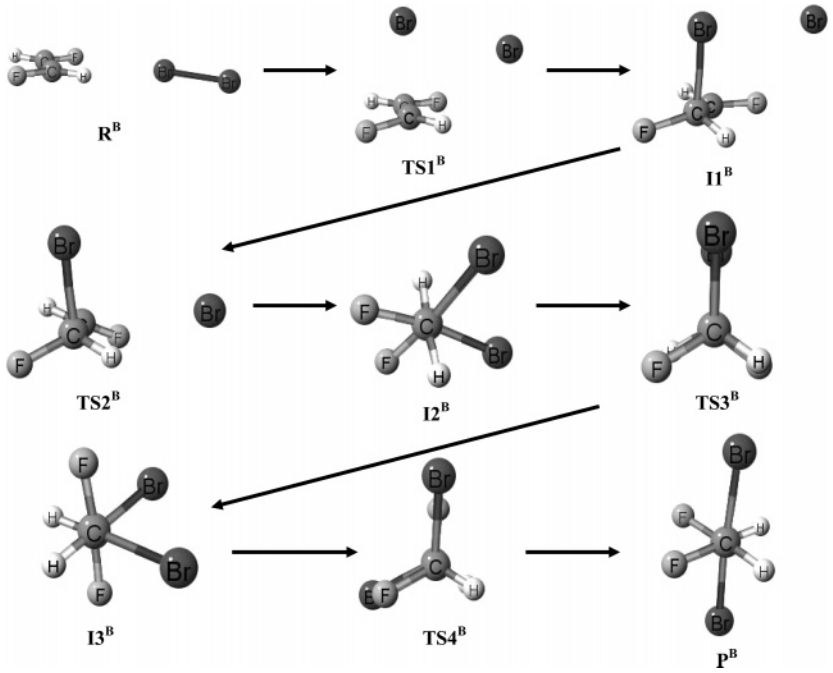

Figure 4. Mechanism for the reaction of (*E*)-CHF═CHF + Br_2 (pathway B). Similar structures are found for the bromination of (*E*)-CHCl═CHCl.

TABLE 3: Activation Energies, Free Energies, and Enthalpies of Activation (kJ mol^{-1}) at 298.15 K for the Reaction of (*E*)-CHF═CHF and (*E*)-CHCl═CHCl with Br_2 (Pathway B)[a,c]

	HF/BC6-31G(d)	MP2/BC6-31G(d)	B3LYP/BC6-31G(d)	G3MP2B3 (BC)
	(*E*)-CHF═CHF + Br_2 → CHFBr−CHFBr			
$\Delta E_{a,TS1}{}^B$	331.8	220.1	197.3	286.4
$\Delta G^{\ddagger}_{TS1}{}^B$	344.5	231.2	206.1	296.0
$\Delta H^{\ddagger}_{TS1}{}^B$	328.2	217.5	193.5	283.4
$\Delta E_{a,TS2}{}^B$	*b*	53.5	9.6	69.0
$\Delta G^{\ddagger}_{TS2}{}^B$	*b*	55.8	10.0	71.9
$\Delta H^{\ddagger}_{TS2}{}^B$	*b*	50.6	5.5	67.3
$\Delta E_{a,TS3}{}^B$	30.4	29.8	25.7	25.8
$\Delta G^{\ddagger}_{TS3}{}^B$	31.2	30.5	26.7	29.4
$\Delta H^{\ddagger}_{TS3}{}^B$	27.6	26.9	22.7	23.6
$\Delta E_{a,TS4}{}^B$	35.4	35.6	27.8	30.7
$\Delta G^{\ddagger}_{TS4}{}^B$	38.5	40.0	31.0	34.2
$\Delta H^{\ddagger}_{TS4}{}^B$	33.1	32.9	25.3	28.4
	(*E*)-CHCl═CHCl + Br_2 → CHClBr−CHClBr			
$\Delta E_{a,TS1}{}^B$	357.1	217.1	215.8	233.8
$\Delta G^{\ddagger}_{TS1}{}^B$	371.8	231.8	223.5	242.7
$\Delta H^{\ddagger}_{TS1}{}^B$	353.0	214.8	211.8	230.9
$\Delta E_{a,TS2}{}^B$	16.5	80.6	42.4	91.9
$\Delta G^{\ddagger}_{TS2}{}^B$	16.6	78.7	40.1	92.1
$\Delta H^{\ddagger}_{TS2}{}^B$	13.9	77.7	38.9	90.8
$\Delta E_{a,TS3}{}^B$	28.9	31.4	24.1	27.9
$\Delta G^{\ddagger}_{TS3}{}^B$	33.0	33.4	26.6	32.0
$\Delta H^{\ddagger}_{TS3}{}^B$	27.0	29.2	22.0	25.6
$\Delta E_{a,TS4}{}^B$	59.6	59.6	50.3	50.8
$\Delta G^{\ddagger}_{TS4}{}^B$	62.9	62.3	53.7	54.7
$\Delta H^{\ddagger}_{TS4}{}^B$	57.0	56.7	47.5	48.5

[a] Mechanistic pathway as defined in Figure 4. [b] Indicates missing values due to failure to optimize the transition state. [c] The products are all in a trans conformation.

3.1.1. Perpendicular Attack of Br_2 to C═C: Pathway A. Although this pathway has been investigated previously,[29,30] the studies involved the reaction of ethene with a single Br_2. The structures of pathway A, perpendicular attack of Br_2 on the C═C bond, along with the relative energies of reactants, transition states, intermediates, and products are shown in Figure 1 for ethene + Br_2. Similar structures are also observed for the reaction of Br_2 with propene, isobutene, fluoroethene, chloroethene, (*E*)-1,2-difluoroethene, and (*E*)-1,2-dichloroethene and are not shown here.

The first step is the formation of a weak alkene/Br_2 (R^A) T-shaped charge-transfer complex with the Br_2 molecule perpendicular to the C═C bond. In all cases, the transition state structure, which is only found at the MP2 level of theory, also retains the T-shaped structure. The transition state ($TS1^A$) involves the rupture of the Br−Br bond and the formation of two C−Br bonds. In the reactant complex R^A, the Br−Br bond distance at the MP2/BC6-31G(d) level of theory is 2.347 Å, while in TS^A it increases to 4.339 Å. However, the C−Br bond distances decrease from 2.962 to 2.906 Å. The IRC analysis confirmed that TS^A leads to R^A and to the bromonium/bromide ion complex, I^A. However, optimization of I^A failed for both the gas phase and in CCl_4 for all alkenes investigated. However, an optimized structure for I^A was obtained in H_2O solution. The activation energies for the reaction of Br_2 with ethene, propene, isobutene, fluoroethene, chloroethene, (*E*)-1,2-difluoroethene, and (*E*)-1,2-dichloroethene in pathway A are listed in Table 1. In all cases, the activation energies ($\Delta E_{a,TS}{}^A$), free energies ($\Delta G^{\ddagger}_{TS}{}^A$), and enthalpies ($\Delta H^{\ddagger}_{TS}{}^A$) of activation are relatively high. Activation energies range from 254.9 to 268.5 kJ mol^{-1} at the MP2/G3MP2large//MP2(FULL)/6-31G(d) level of theory. This pathway does not lead to *trans*-1,2-dibromoalkane, which is known[22] to be the product of most simple alkenes.

3.1.2. Sidewise Attack of Br_2 to C═C: Pathway B. The structures for pathway B are shown in Figure 2 for the reaction of ethene and Br_2. Similar structures are also observed for the reaction of Br_2 with propene, isobutene, fluoroethene, and chloroethene. The relative energies of reactants, intermediates, transition states, and products are shown in Figure 3. Activation energies, free energies, and enthalpies of activation for the reaction of Br_2 with ethene, propene, isobutene, fluoroethene, and chloroethene are given in Table 2.

In addition to the previously reported CTC, R^A, a second alkene/Br_2 complex (R^B) was found. For the ethene/Br_2 and propene/Br_2 complexes, the perpendicular complex is more stable by 9.0 and 12.8 kJ mol^{-1} at the G3MP2B3 level, respectively. Unlike pathway A, with few exceptions, the structures exist at all levels of theory and basis sets investigated

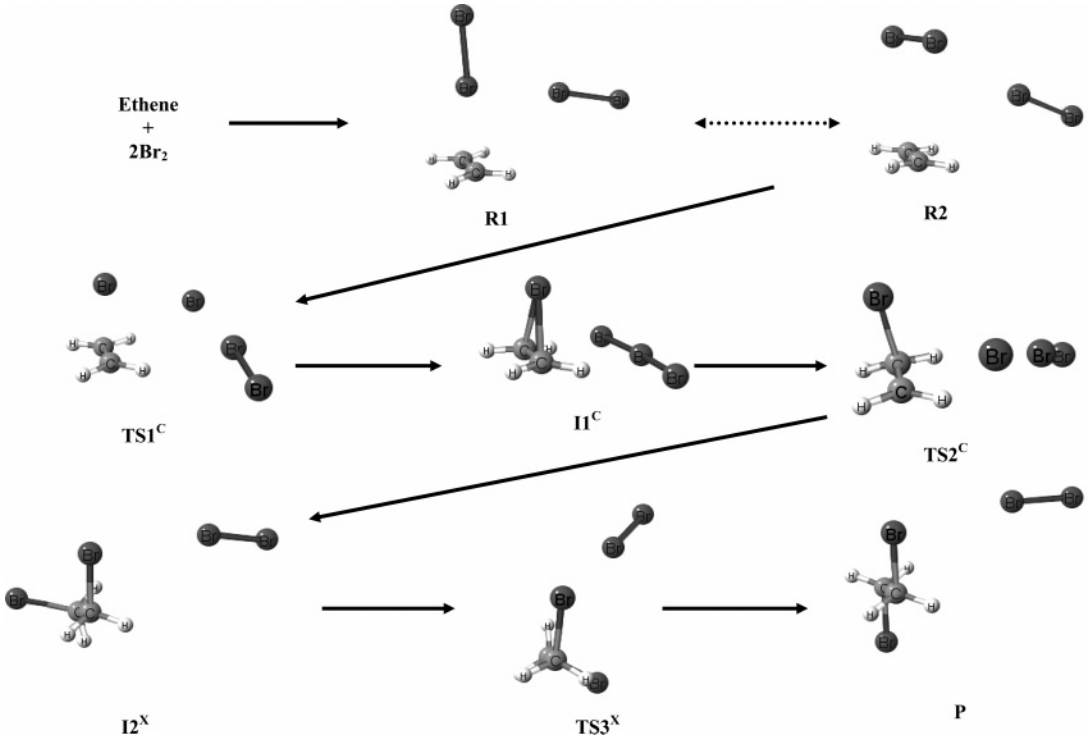

Figure 5. Mechanism for the reaction of $CH_2{=}CH_2 + 2Br_2$ (pathway C).

in this case. Pathway B is a multiple-step process. In the first step, a bromonium ion/Br^- intermediate $I1^B$ is formed via $TS1^B$. For ethene, the Br−Br bond distance in the reactant complex R^B is 2.311 Å at the MP2/BC6-31G(d) level of theory, while in $TS1^B$ the distance increases to 2.963 Å. The IRC analysis confirmed that $TS1^B$ leads to R^B and $I1^B$. The activation energies, free energies, and enthalpies of activation calculated using the BC6-31G(d) and standard 6-31G(d) basis set are very similar at all the levels of theory (Table 2). Due to convergence failure in the QCISD(T) calculation, no G3 results were obtained for the reaction of Br_2 with ethene and propene. However, for isobutene the QCISD(T) did converge, and the activation energies obtained at the MP2/BC6-31G(d) and G3MP2B3 levels are found to be within 1.9 kJ mol^{-1}. Hence, the activation energies at the MP2/BC6-31G(d) level of theory should agree well with G3 theories for the first step of pathway B. Inclusion of a larger basis set does not change the barrier significantly (Table 2). The activation energies for the reaction of Br_2 with ethene and propene are 247.3 and 200.4 kJ mol^{-1} at the MP2/BC6-31G(d) level of theory, respectively. Although it was observed that the IRC leads from $TS1^B$ to R^B and $I1^B$ for all DFT methods, for some functionals no structure for $I1^B$ was found. All attempts at optimizing the intermediate $I1^B$ converged to the *trans*-1,2-dibromoalkane product. For the reaction of ethene and propene, optimized structures for $I1^B$ were obtained with B3PW91/BC6-31G(d) and B3P86/BC6-31G(d) levels of theory. It was also possible to obtain an optimized structure for $I1^B$ in the case of ethene at the B3LYP/BC6-31G(d) level by decreasing the default maximum step size in the optimization from MaxStep = 30 to MaxStep = 1. For cases in which no DFT structures for $I1^B$ were obtained, single-point calculations were performed using MP2/6-31G(d) geometries (Table 2). In the second step of pathway B, a gauche dibromoalkane intermediate ($I2^B$) is formed via $TS2^B$. The corresponding activation energy ($\Delta E_{a.TS2}{}^B$) at G3MP2B3 for propene is 37.0 kJ mol^{-1}, which again agrees very well with the MP2/BC6-31G(d) (45.0 kJ mol^{-1}) level of theory. Similar agreement is also expected for the other alkenes. The activation energies

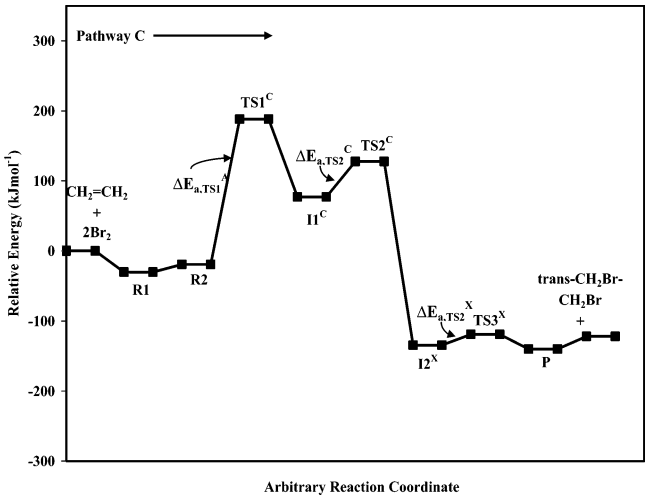

Figure 6. Pathway for the reaction of $CH_2{=}CH_2 + 2Br_2$ (pathway C) at the G3MP2B3 level of theory (see Figure 5 for structures).

($\Delta E_{a.TS2}{}^B$) for the reaction of Br_2 with ethene and isobutene are 58.3 and 54.2 kJ mol^{-1} at MP2/BC6-31G(d), respectively. Finally, the *trans*-1,2-dibromoalkane product (P^B), a conformational isomer of $I2^B$, is formed via $TS3^B$, which involves rotation about the C−C bond with activation energies of 13.9 and 22.0 kJ mol^{-1} for (*E*)-1,2-dibromoethene and (*E*)-1,2-dibromopropene, respectively at G3MP2B3. Solvation (CCl_4) has no effect on the reaction mechanism at the MP2/6-31G(d) and B3LYP/6-31G(d) levels of theory. The solvent model used in this study predicts the free energies of activation for the rate-determining step to be 262.9 and 191.0 kJ mol^{-1} at MP2/6-31G(d) and B3LYP/6-31G(d), respectively, for ethene and 233.5 and 165.9 kJ mol^{-1} at MP2/6-31G(d) and B3LYP/6-31G(d), respectively, for propene.

In the cases of fluoro- and chloroethene, Br_2 can attack from two different directions (syn and anti). For syn attack (substituent side), the activation energies ($\Delta E_{a.TS1}{}^B$) are 224.2 and 206.1 kJ

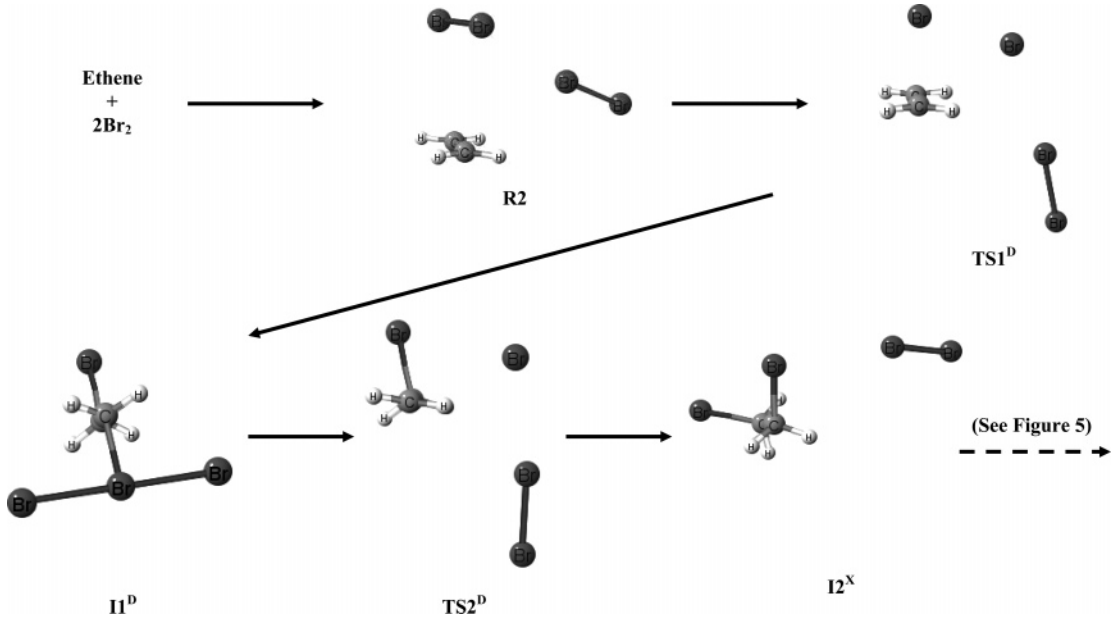

Figure 7. Mechanism for the reaction of $CH_2{=}CH_2 + 2Br_2$ (pathway D).

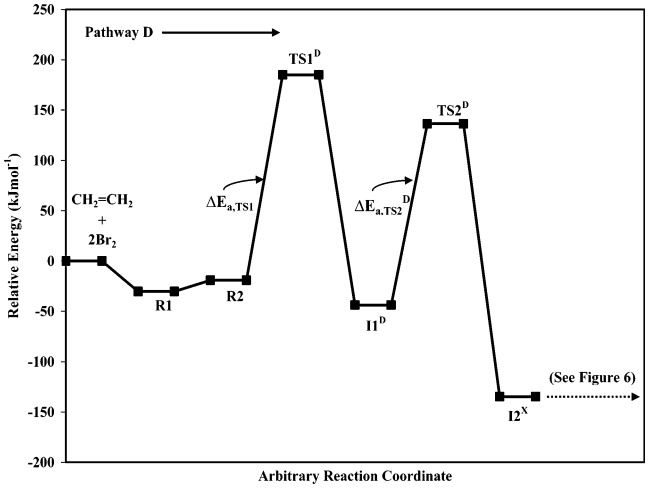

Figure 8. Pathway for the reaction of $CH_2{=}CH_2 + 2Br_2$ (pathway D) at the G3MP2B3 level of theory (see Figure 7 for structures).

mol^{-1} for F and Cl, respectively, at the MP2/BC6-31G(d) level of theory, whereas for anti attack the activation energies are 238.4 and 240.1 kJ mol^{-1} for F and Cl, respectively. The activation energies ($\Delta E_{a.TS2}{}^{B}$) in step two of the Br_2 reaction with fluoroethene and chloroethene are 33.6 and 6.8 kJ mol^{-1} at the MP2/BC6-31G(d) level for syn addition and 23.0 and 27.2 kJ mol^{-1} for anti addition. The last step involves rotation around the C−C bond with all of the levels predicting a low barrier (Table 2). The barriers for the rate-determining step decrease in the order ethene > fluoroethene > chloroethene > propene > isobutene with values of 247.3, 224.2, 206.1, 200.4, and 189.3 kJ mol^{-1} at the MP2/BC6-31G(d) level, respectively. This is consistent with experiment[44,45] where the relative rates of bromination follow the order $(CH_3)_2C{=}C(CH_3)_2 > CH_3CH_2{-}CH{=}CH_2 > CH_2{=}CH_2$.

Reaction of Br_2 with (*E*)-1,2-difluoroethene and (*E*)-1,2-dichloroethene is a four-step process. The corresponding activation energies, free energies, and enthalpies of activation are given in Table 3. All of the structures for this mechanism are shown in Figure 4.

The activation energies of the rate-determining step are 220.1 kJ mol^{-1} for (*E*)-1,2-difluoroethene and 217.1 kJ mol^{-1} for (*E*)-1,2-dichloroethene at MP2/BC6-31G(d). The corresponding activation energies for step two are 69.0 and 91.9 kJ mol^{-1}. Intermediate $I3^B$, a rotamer of $I2^B$, is formed via $TS3^B$, with activation energies of 25.8 and 27.9 kJ mol^{-1} at G3MP2B3 for 1,2-diflouroethene and dichloroethene, respectively. Similarly, product P^B, which is also a conformational isomer of $I3^B$, is

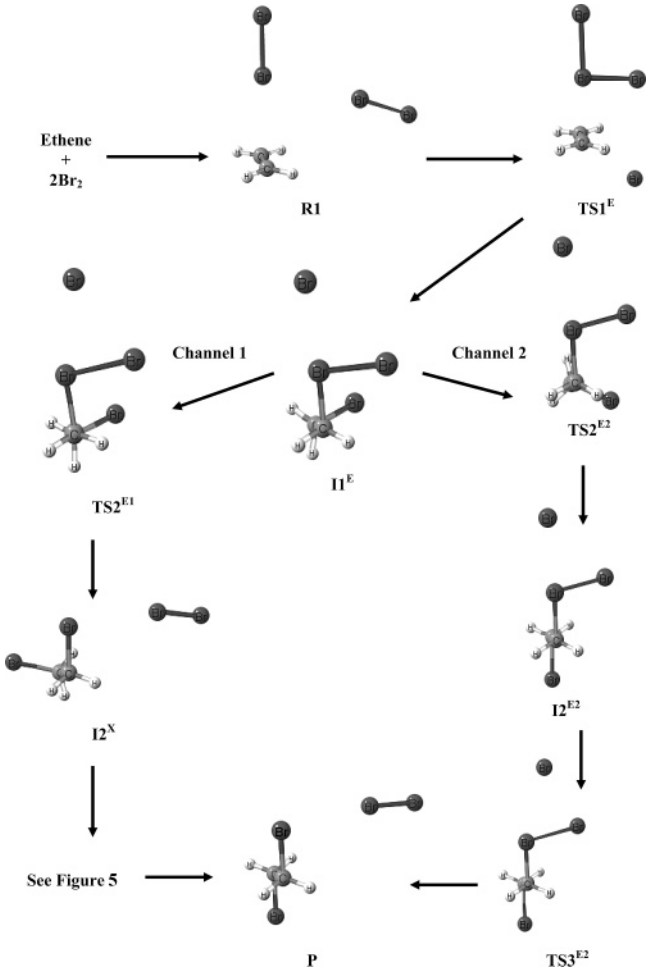

Figure 9. Mechanism for the reaction of $CH_2{=}CH_2 + 2Br_2$ (pathway E).

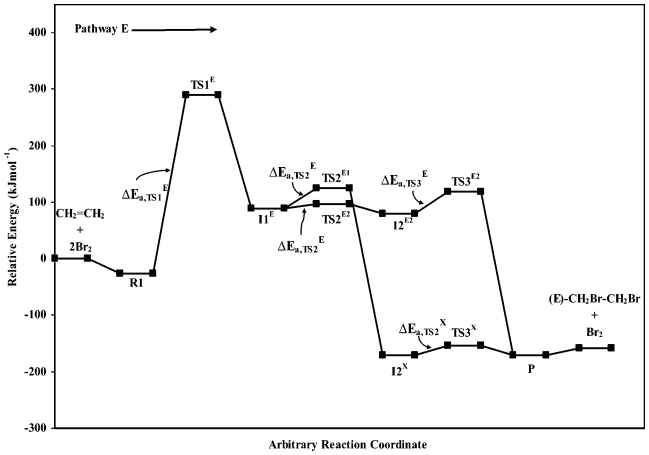

Figure 10. Pathway for the reaction of $CH_2{=}CH_2 + 2Br_2$ (pathway E) at the MP2/G3MP2large//HF/6-31G(d) level of theory (see Figure 9 for structures).

formed via $TS4^B$, with activation energies of 30.7 and 50.8 kJ mol^{-1} at G3MP2B3 for diflouro- and dichloroethene, respectively.

3.2. Potential Energy Surfaces for the Reaction of Ethene with $2Br_2$. In this case, we investigate pathways for the reaction with ethene only. The results for the reaction of ethene and $2Br_2$ will be discussed in the following order: (1) pathway C, (2) pathway D, (3) pathway E, and (4) pathway F. For pathways C and D and channel 1 of pathway E, intermediate $I2^X$ and $TS3^X$ are labeled as X because they are common to these pathways.

3.2.1. Pathway C. The structures of reactants, intermediates, transitions states, and products of pathway C are shown in Figure 5. The relative energies of reactants, intermediates, transition states, and products are shown in Figure 6. Activation energies, free energies, and enthalpies of activation for pathway C are given in Table 4.

Ethene + $2Br_2$ can form two possible complexes, R1 and R2. Complex R2 reacts through $TS1^C$ to form intermediate $I1^C$, which is a bromonium/tribromide ion pair. The Br−Br bond distance in the Br_2 adding to C═C goes from 2.302 Å in the R2 complex to 2.940 Å in $TS1^C$ at MP2/6-31G(d). The IRC analysis confirmed that $TS1^C$ leads to R2 and $I1^C$. The activation energy ($\Delta E_{a.TS1}{}^C$) is 207.3 kJ mol^{-1} at the G3MP2B3 level. MP2 appears to overestimate while DFT appears to be underestimating the barrier for this reaction. The activation energy ($\Delta E_{a.TS1}{}^C$) obtained by MP2/6-31G(d) is higher than the G3MP2B3 value by 25.5 kJ mol^{-1}, while the activation energies obtained by B3LYP are lower by 47.0 and 39.5 kJ mol^{-1} at 6-31G(d) and 6-31+G(d), respectively. However, activation energies do not depend significantly on the choice of basis set. Activation energies at MP2/6-31G(d) (232.8 kJ mol^{-1}) and at MP2/G3MP2large//B3LYP/6-31G(d) (232.1 kJ mol^{-1}) differ by only 0.7 kJ mol^{-1}, and B3LYP/6-31G(d) (160.3 kJ mol^{-1}) and B3LYP/6-31+G(d) (167.8 kJ mol^{-1}) differ by only 7.5 kJ mol^{-1}. The activation energies, free energies, and enthalpies of activation calculated using the BC6-31G(d) bromine basis set and the standard 6-31G(d) basis set are also found to be very similar at all levels of theory (Table 4). In the next step, intermediate $I2^X$ is formed via $TS2^C$, where a Br atom from Br_3^- attacks the bromonium ion, resulting in a gauche 1,2-dibromoethane/Br_2 complex. The corresponding activation energy ($\Delta E_{a.TS2}{}^C$) is 50.7 kJ mol^{-1} at G3MP2B3. The activation energy obtained by MP2/6-31G(d) (55.1 kJ mol^{-1}) again gives the best agreement with G3MP2B3. Finally, the product, *trans*-1,2-dibromoethane (P), is formed via transition state $TS3^X$, which involves rotation about the C−C bond. The activation energy for this last step ($\Delta E_{a.TS3}{}^X$) is 15.6 kJ mol^{-1} at G3MP2B3. All structures for pathway C were also obtained for the reaction in CCl_4 solution at MP2/6-31G(d). The free energy of activation for the rate-determining step in CCl_4 decreases by 7.9 kJ mol^{-1}.

3.2.2. Pathway D. The structures of pathway D are shown in Figure 7. The relative energies of reactants, intermediates, transitions states, and products are shown in Figure 8. Activation energies, free energies, and enthalpies of activation are given in Table 5.

The first step of pathway D involves formation of an interesting stable intermediate, *trans*-1-bromo-2-tribromoethane ($I1^D$). $I1^D$ is formed via transition state $TS1^D$, with an activation energy ($\Delta E_{a.TS1}{}^D$) of 204.3 kJ mol^{-1} at the G3MP2B3 level. In $TS1^D$ one Br atom adds to one of the C atoms of C═C, while Br_3^- adds to the other C, resulting in a trans configuration. (Figure 7). The IRC analysis confirmed that $TS1^D$ leads to R2 and $I1^D$. Intermediate $I1^D$ is converted to intermediate $I2^X$ via $TS2^D$, with an activation energy of 180.2 kJ mol^{-1} at the G3MP2B3 level of theory. The transition state ($TS2^D$) structure consists of two bond ruptures (Br−Br and C−Br) and one bond formation (C−Br). The last step, $I2^X \rightarrow P$ is the same as for pathway C (Figures 5 and 6). A similar mechanism is found in CCl_4 solution for this reaction. The solvent model used in this study predicts that the free energy of activation for this pathway would be reduced in CCl_4. For the rate-determining step, $\Delta G^{\ddagger}$ is lowered by 9.4 and 15.4 kJ mol^{-1} at the MP2/6-31G(d) and B3LYP/6-31G(d) levels, respectively.

3.2.3. Pathway E. The geometries for the reactants, intermediates, transition states, and products involved in pathway E are shown in Figure 9. The relative energies of reactants, intermediates, transition states, and products for pathway E are shown in Figure 10. The activation energies, free energies of activation, and enthalpies of activation are given in Table 6.

Pathway E involves a perpendicular attack by one Br_2 and a sidewise attack by the other Br_2 ($TS1^E$), which leads to intermediate $I1^E$ (Figure 9). $I1^E$ can lead to product P through two different channels (1 and 2). The first step of pathway E and the first step of channel 1 are only obtained at the HF level of theory. However, the activation energies for the first step of this pathway are extremely high (476.0 and 315.6 kJ mol^{-1} at the HF/6-31G(d) and MP2/G3MP2large//HF/6-31G(d) levels of theory, respectively). The results are simply presented here for completeness.

3.2.4. Pathway F. The structures of reactants, intermediates, transitions states, and products of pathway F are shown in Figure 11. The relative energies of reactants, intermediates, transition states, and products are shown in Figure 12. The activation energies, free energies, and enthalpies of activation for the first step of pathway F and for the overall reaction are given in Table 7.

All of the optimized structures of pathway F were obtained at the HF level, except for $TS1^F$, despite several attempts. It was possible to obtain an optimized structure for $TS1^F$ using MP2 and B3LYP. In addition to the two reactant complexes R1 and R2, a third ethene/$2Br_2$ complex (R3) was found. For the ethene/$2Br_2$ complexes, R1 and R3 have one Br_2 perpendicular to C═C, and both R1 and R3 are energetically more stable than R2. Pathway F is a multiple-step process. In the first step, complex R3 reacts through $TS1^F$ to form intermediate $I1^F$. In R3 the Br−Br bond distance for the Br_2 attacking C═C is 2.345 Å at the MP2/BC6-31G(d) level of theory while it increases to 2.815 Å in $TS1^F$. The IRC analysis at the MP2 and

TABLE 4: Activation Energies, Free Energies, and Enthalpies of Activation (kJ mol^{-1}) at 298.15 K for the Reaction of CH_2=CH_2 and $2Br_2$ (Pathway C)[a]

level/basis set	$\Delta E_{a,TS1}{}^{C}$	$\Delta G^{\ddagger}_{TS1}{}^{C}$	$\Delta H^{\ddagger}_{TS1}{}^{C}$	$\Delta E_{a,TS2}{}^{C}$	$\Delta G^{\ddagger}_{TS2}{}^{C}$	$\Delta H^{\ddagger}_{TS2}{}^{C}$	$\Delta E_{a,TS3}{}^{X}$	$\Delta G^{\ddagger}_{TS3}{}^{X}$	$\Delta H^{\ddagger}_{TS3}{}^{X}$
HF/6-31G(d)	301.2	324.9	302.0	35.1	36.9	31.7	12.2	20.1	7.6
HF/BC6-31G(d)	284.4	304.3	282.6	34.5	30.8	30.0	16.1	17.8	13.9
MP2/6-31G(d)	232.8	260.8	230.7	55.1	52.6	51.2	17.1	18.2	14.8
CCl_4[c]		252.9			64.3			18.4	
MP2/BC6-31G(d)	*b*	*b*	*b*	50.6	51.5	46.8	17.6	18.9	15.1
B3LYP/6-31G(d)	160.3	180.7	160.5	31.0	26.0	27.0	14.7	16.9	12.5
B3LYP/BC6-31G(d)	157.4	175.2	154.3	31.4	30.0	27.5	14.9	18.6	12.5
B3LYP/6-31+G(d)	167.8	207.5	165.7	31.3	23.8	27.2	14.7	15.9	12.5
B3LYP/BC6−31+G(d)	160.8	181.3	158.4	32.9	32.2	29.2	15.4	21.7	10.3
MP2/G3MP2large //B3LYP/6-31G(d)	232.1	249.8	229.5	69.7	68.6	69.5	17.7	20.5	16.0
G3MP2B3	207.3	224.9	204.7	50.7	49.6	50.5	15.6	18.4	13.9

[a] Barriers as defined in Figures 5 and 6. [b] Indicates missing values due to failure to optimize the transition state. [c] The PCM-UA0 model was used for optimized structures. In all cases $\Delta G = \Delta\Delta G$ (thermal correction) + ΔG_{solv}.

TABLE 5: Activation Energies, Free Energies and Enthalpies of Activation (kJ mol^{-1}) at 298.15 K for the Reaction of CH_2=CH_2 and $2Br_2$ (Pathway D)[a]

level/basis set	$\Delta E_{a,TS1}{}^{D}$	$\Delta G^{\ddagger}_{TS1}{}^{D}$	$\Delta H^{\ddagger}_{TS1}{}^{D}$	$\Delta E_{a,TS2}{}^{D}$	$\Delta G^{\ddagger}_{TS2}{}^{D}$	$\Delta H^{\ddagger}_{TS2}{}^{D}$
HF/6-31G(d)	302.0	325.5	302.8	113.0	90.4	103.2
HF/BC6-31G(d)	288.5	305.2	286.4	132.6	114.8	123.2
MP2/6-31G(d)	232.8	260.8	230.7	191.3	177.9	183.4
CCl_4[c]		251.4			151.0	
MP2/BC6-31G(d)	225.6	222.8	238.0	*b*	*b*	*b*
B3LYP/6-31G(d)	160.5	176.3	160.6	148.6	137.1	139.8
CCl_4[c]		160.9			112.1	
B3LYP/BC6-31G(d)	*b*	*b*	*b*	156.6	128.2	147.9
B3LYP/6-31+G(d)	167.8	203.1	165.7	147.1	136.6	138.4
B3LYP/BC6−31+G(d)	*b*	*b*	*b*	158.1	129.4	148.9
MP2/G3MP2large //B3LYP/6-31G(d)	242.6	248.6	232.9	214.2	212.6	215.3
G3MP2B3	204.3	210.3	194.6	180.2	178.5	181.2

[a] Barriers as defined in Figures 7 and 8. [b] Indicates missing values due to failure to optimize the transition state. [c] The PCM-UA0 model was used for optimized structures. In all cases $\Delta G = \Delta\Delta G$ (thermal correction) + ΔG_{solv}.

TABLE 6: Activation Energies, Free Energies, and Enthalpies of Activation (kJ mol^{-1}) at 298.15 K for the Reaction of CH_2=CH_2 and $2Br_2$ (Pathway E)[a,b]

level/basis set	$\Delta E_{a,TS1}{}^{E}$	$\Delta G^{\ddagger}_{TS1}{}^{E}$	$\Delta H^{\ddagger}_{TS1}{}^{E}$	$\Delta E_{a,TS2}{}^{E1}$	$\Delta G^{\ddagger}_{TS2}{}^{E1}$	$\Delta H^{\ddagger}_{TS2}{}^{E1}$
HF/6-31G(d)	476.0	509.8	473.9	45.9	44.3	43.5
CCl_4[c]		404.4[d]			79.2	
HF/BC6-31G(d)	470.1	490.0	467.4	44.9	43.0	42.5
MP2/G3MP2large //HF/6-31G(d)	315.6	346.3	310.1	35.4	35.3	34.2

	$\Delta E_{a,TS2}{}^{E2}$	$\Delta G^{\ddagger}_{TS2}{}^{E2}$	$\Delta H^{\ddagger}_{TS2}{}^{E2}$	$\Delta E_{a,TS3}{}^{E2}$	$\Delta G^{\ddagger}_{TS3}{}^{E2}$	$\Delta H^{\ddagger}_{TS3}{}^{E2}$
HF/6-31G(d)	7.6	11.1	5.4	47.7	44.9	45.0
HF/BC6-31G(d)	10.1	13.5	8.1	46.3	43.7	43.8
MP2/BC6-31G(d)	10.8	14.0	8.2	10.9	9.7	9.2
B3LYP/BC6-31G(d)	8.7	11.9	6.3	20.4	20.5	18.0
B3LYP/BC6−31+G(d)	8.9	10.9	6.3	18.1	18.7	15.8
MP2/G3MP2large //HF/6-31G(d)	7.4	4.0	−2.0	38.9	38.0	37.9

[a] Barriers as defined in Figures 9 and 10. [b] $TS1^E$ and $TS2^{E1}$ were only obtained at HF/6-31G(d) and HF/BC6-31G(d). [c] The PCM-UA0 model was used for optimized structures. In all cases $\Delta G = \Delta\Delta G$ (thermal correction) + ΔG_{solv}. [d] Have two imaginary frequencies; the smallest one is 14.98 cm^{-1}.

B3LYP levels confirmed that $TS1^F$ leads to R3 and $I1^F$. The activation energy ($\Delta E_{a,TS1}{}^{F}$) is 119.0 kJ mol^{-1} at the G3MP2B3 level. Intermediate $I1^F$ can also form from the direct attack by a Br_4 molecule to ethene. However, the activation energy for the formation of Br_4 ($Br_2 + Br_2 \rightarrow Br_4$) (Figure 13) is high (174.6 kJ mol^{-1} at G3MP2B3). Therefore, ethene will more likely react with $2Br_2$ than Br_4. All of the optimized structures from $TS1^F$ to $TS3^F$ (the last step) of pathway F involve bromonium/Br_3^- ion pairs all very close in energy (Figure 12). However, $TS3^F$ has a slightly higher energy than $TS1^F$ (7 kJ mol^{-1} at G3MP2B3(BC)). In the second step, $I2^F$ is formed via $TS2^F$ with an activation energy ($\Delta E_{a,TS2}{}^{F}$) of only 2 kJ mol^{-1} at the HF/BC6-31G(d) level. Optimization of $TS2^F$, $I2^F$, and $I3^F$ failed with MP2 and B3LYP. The structure of intermediate $I2^F$ is very similar to intermediate $I3^F$ with the only difference being in the position of Br_3^-. Finally, the product (P) is formed via transition state $TS3^F$, which involves one C−Br bond rupture from the bromonium ion and a trans addition of Br from Br_3^-

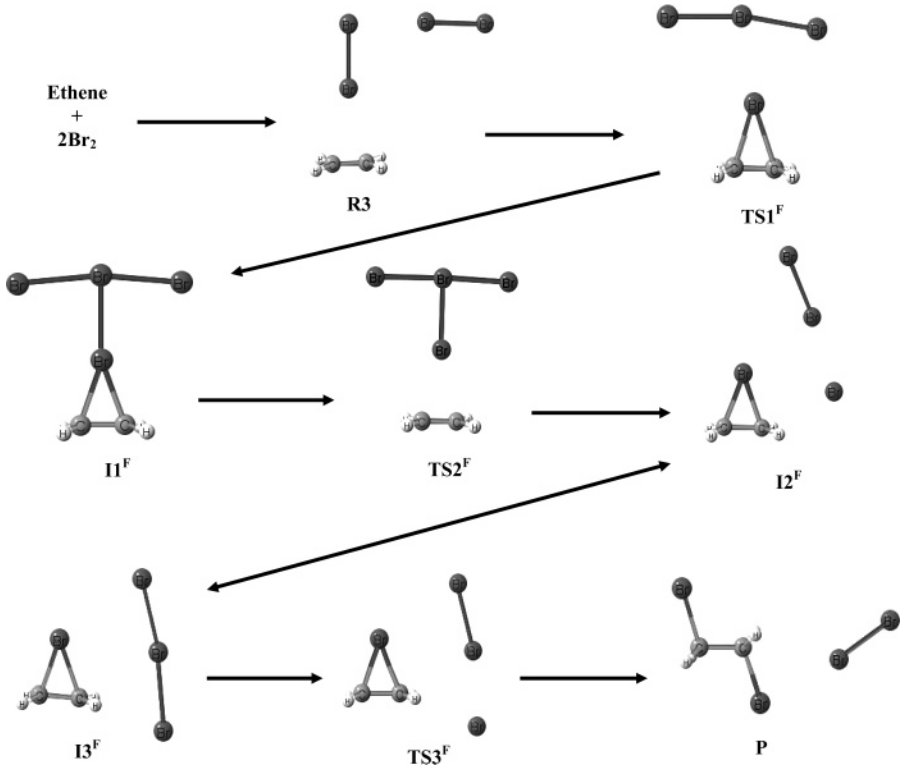

Figure 11. Mechanism for the reaction of $CH_2{=}CH_2 + 2Br_2$ (pathway F).

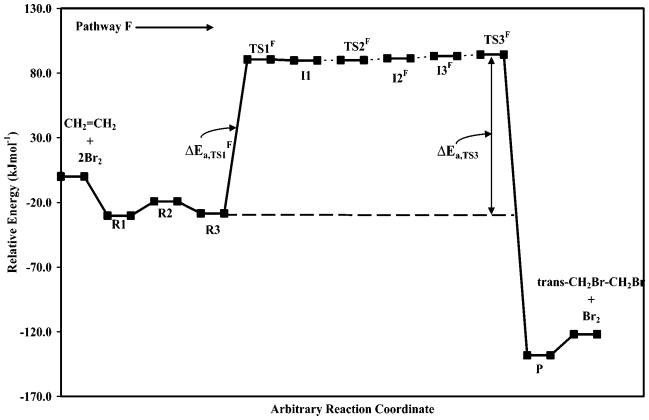

Figure 12. Pathway for the reaction of $CH_2{=}CH_2 + 2Br_2$ (pathway F) at the G3MP2B3 level of theory (see Figure 11 for structures). For $TS2^F$, $I2^F$, and $I3^F$ the G3MP2B3 energies are calculated using HF/6-31G(d) optimized geometries.

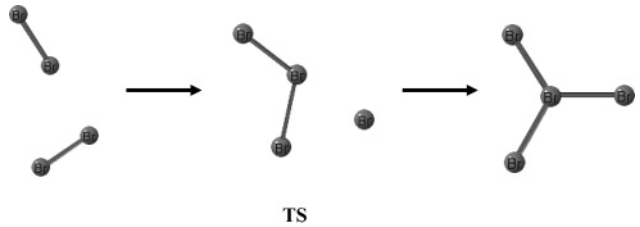

Figure 13. Mechanism for the reaction of $Br_2 + Br_2 \rightarrow Br_4$.

to the C. The IRC analysis confirmed that $TS3^F$ leads to $I3^F$ and P for all levels of theory. However, optimization of $I3^F$ leads to reactant complex R3 at both MP2 and B3LYP. It has been found that the overall activation energy ($\Delta E_{a.TS3}{}^F$) calculated from R3 to $TS3^F$ is higher than the activation energy of the first step ($\Delta E_{a.TS1}{}^F$) in pathway F for all levels of theory (Table 7). The overall reaction barriers in pathway F are 151.9, 111.6, 101.8, and 122.7 kJ mol^{-1} at the HF/BC6-31G(d), MP2/BC6-31G(d), B3LYP/BC6-31G(d), and G3MP2B3 levels of theory, respectively. Unlike other pathways, the overall activation energy obtained at MP2 agrees well with that obtained at B3LYP. The activation energies, free energies, and enthalpies of activation calculated using the BC6-31G(d) and standard 6-31G(d) basis sets differ by no more than 15.4 kJ mol^{-1} ($\Delta H^{\ddagger}_{TS1}{}^F$), and it is interesting to note that the B3LYP/6-31G(d) and MP2/BC6-31G(d) results are in excellent agreement (Table 7). Structures similar to those in the gas phase were also obtained in CCl_4 solution at the MP2 and B3LYP levels. The overall free energy of activation in CCl_4 (Table 8) decreases by 49.7 and 32.7 kJ mol^{-1} at the MP2/BC6-31G(d) and B3LYP/BC6-31G(d) levels from that of the gas phase.

3.3. Summary of Overall Reaction Mechanisms Investigated. The most likely mechanism for the reaction of alkenes with one Br_2 is pathway B. The activation energies of the rate-determining step of pathway B for the reaction with ethene, propene, isobutene, flouroethene, chloroethene, (*E*)-1,2-difluoroethene, and (*E*)-1,2-dichloroethene are 247.3, 200.4, 189.3, 224.2, 206.1, 220.1, and 217.1 kJ mol^{-1}, respectively, at the MP2/BC6-31G(d) level of theory, while the barriers for pathway A are 256.4, 249.8, 244.8, 247.6, 244.9, 243.4, and 249.3 kJ mol^{-1}, respectively. For the reaction of $2Br_2$ with ethene, pathways C and D have almost the same barrier for the rate-determining step with G3MP2B3 activation energies of 207.3 and 204.4 kJ mol^{-1}, respectively. Pathway E is predicted to have a high activation energy (315.6 kJ mol^{-1} at MP2/G3MP2large//HF/6-31G(d)). The most likely mechanism for the reaction of ethene with $2Br_2$ is pathway F with an overall barrier of 122.7 kJ mol^{-1} at G3MP2B3. By comparison of the most likely pathway for the reaction with one Br_2 (pathway B) and most likely pathway for the reaction with two Br_2 (pathway F), bromination should be mediated via $2Br_2$ where the second Br_2 assists in the ionization of the reactant complex to form a bromonium/Br_3^- ion pair.

TABLE 7: Activation Energies, Free Energies, and Enthalpies of Activation (kJ mol^{-1}) at 298.15 K for the Reaction of CH_2=CH_2 and $2Br_2$ (Pathway F)[a]

level/basis set	$\Delta E_{a,TS1}{}^F$	$\Delta G^{\ddagger}_{TS1}{}^F$	$\Delta H^{\ddagger}_{TS1}{}^F$	$\Delta E_{a,TS3}{}^F$	$\Delta G^{\ddagger}_{TS3}{}^F$	$\Delta H^{\ddagger}_{TS3}{}^F$
HF/BC6-31G(d)	*b*	*b*	*b*	151.9	177.8	155.3
MP2/BC6-31G(d)	103.8	126.0	104.2	111.6	136.8	112.4
B3LYP/BC6-31G(d)	90.5	108.8	89.1	101.8	123.1	100.6
B3LYP/6-31G(d)	103.3	117.0	104.5	110.9	126.6	112.2
B3LYP/BC6−31+G(d)	83.6	99.3	82.2	100.7	119.3	99.7
G3MP2B3	119.0	129.1	116.5	122.7	134.3	119.8
G3MP2B3(BC)	117.5	132.3	112.5	125.6	142.6	119.9

[a] Mechanistic pathway and barriers as defined in Figures 11 and 12, respectively. [b] Indicates missing values due to failure to optimize the transition state.

TABLE 8: Calculated Overall Free Energies of Activation (kJ mol^{-1}) at 298.15 K for the Reaction of CH_2=CH_2 and $2Br_2$ in Solution at B3LYP/BC6-31G(d) (Pathway F) and Experimental Values

solvent (ϵ)[a]	calculated	solvent (ϵ)[a]	experimental
CCl_4 (2.23)	90.4 (87.1)[b]	CH_3COOH (6.15)	76.8[c]
CH_2Cl_2 (8.93)	64.6	CCl_2H-CCl_2H (8.2)	66.4[c]
CH_2Cl-CH_2 Cl (10.36)	52.7	CH_3OH (32.63)	64.6[d] (72.5)[e]
CH_3OH (32.63)	39.2 (75.5)[f]		

[a] In order of increasing dielectric constants (ϵ). [b] The value in parentheses is obtained at the MP2/BC6-31G(d) level of theory. [c] Reference 46. [d] Reference 45. [e] Corrected for solvent concentration. (See text for explanation.) [f] For the reaction of ethene + Br_2 mediated by a CH_3OH molecule in CH_3OH solution.

3.4. Comparison with Experiment. A general kinetic equation for the addition of bromine to alkenes is given as[4]

$$-d[Br_2]/dt = k_2[Br_2][A] + k_3[Br_2]^2[A] + k_3'[Br_3^-][A] \quad (1)$$

where [A] = [alkene].

Modro et al.[46] found that in the absence of bromide ion and at low bromine concentrations ([Br_2] < 10^{-3} M) in CH_3COOH, eq 1 reduces to the form

$$-d[Br_2]/dt = k_2[Br_2][A] \quad (2)$$

and under the same conditions in CCl_2H-CCl_2H a third-order rate dependence was found

$$-d[Br_2]/dt = k_3[Br_2]^2[A] \quad (3)$$

The free energies of activation in CH_3COOH and in CCl_2H-CCl_2H were calculated from the experimental[46] rate constants obtained by eqs 2 and 3. Equation 2 was also used by Dubois and Mouvier[45] to determine the rate constant for the bromination of ethene in CH_3OH. These experimental free energies of activation are given in Table 8.

To compare our findings to experiment, four solvents with increasing polarity were chosen, namely CCl_4, CH_2Cl_2, CH_2Cl-CH_2Cl, and CH_3OH. The calculated overall free energies of activation for the most likely pathway (pathway F) in the reaction of ethene with $2Br_2$ in CCl_4, CH_2Cl_2, CH_2Cl-CH_2Cl, and CH_3OH are also given in Table 8. It has been found that the overall free energies of activation decrease with the increase of polarity of the solvent. The experimental values are also known[47] to decrease with the polarity of solvent. Although the experimental free energies in CH_3COOH, CCl_2H-CCl_2H, and CH_3OH were obtained from two different conditions, they also show decreasing free energies with increasing polarity from CH_3COOH to CH_3OH (Table 8). The calculated free energy of activation for the reaction of ethene with $2Br_2$ in CH_2Cl_2 is in excellent agreement with the experimental value obtained in CCl_2H-CCl_2H, differing by only 1.8 kJ mol^{-1} at B3LYP/BC6-31G(d). In this case, the two solvents, CH_2Cl_2 and CCl_2H-CCl_2H, have almost identical dielectric constants with values of 8.93 and 8.2, respectively. Similarly, the calculated activation energy in CH_2Cl-CH_2Cl (52.7 kJ mol^{-1}) and the experimental activation energy in CCl_2H-CCl_2H (66.4 kJ mol^{-1}) differ by only 13.7 kJ mol^{-1} where the dielectric constant for CH_2Cl-CH_2Cl is 10.36 vs 8.2 for CCl_2H-CCl_2H. As expected, a more polar solvent would result in a lower $\Delta G^{\ddagger}$. It is worth mentioning here that the solvent models for CCl_2H-CCl_2H have not yet been implemented in Gaussian 03, and hence CH_2Cl-CH_2Cl and CH_2Cl_2 solvents were used in this study because these two solvents have almost similar structural features and dielectric constants compared to CCl_2H-CCl_2H.

The experimental free energy of activation obtained from the rate constant for the bromination of ethene in methanol is 64.6 kJ mol^{-1} and found to be first order in Br_2.[45] This barrier is significantly higher than the computed free energy of activation for the reaction with $2Br_2$ (39.2 kJ mol^{-1} at B3LYP/BC6-31G(d)). This disagreement may be explained in a number of ways. One possibility is that perhaps due to the relatively high polarity of CH_3OH (dielectric constant of 32.63) both Br_2 and $2Br_2$ mechanisms occur simultaneously and the observed experimental free energy values would correspond to an average of the two. Alternatively and more likely, the mechanism in polar protic solvents may be different. We propose the following two cases: Case 1

$$A + Br_2 \underset{k_{-1}}{\overset{k_1}{\rightleftharpoons}} R2$$

$$R2 + X \underset{k_{-2}}{\overset{k_2}{\rightleftharpoons}} R3$$

$$R3 \xrightarrow{k_3} P$$

Case 2

$$Br_2 + X \underset{k_{-1}}{\overset{k_1}{\rightleftharpoons}} Br_2X$$

$$Br_2X + A \underset{k_{-2}}{\overset{k_2}{\rightleftharpoons}} R3$$

$$R3 \xrightarrow{k_3} P$$

where X can be Br_2 or a solvent molecule.

Both cases lead to the same rate expression

$$\frac{dP}{dt} = \frac{k_1k_2k_3}{k_{-1}k_{-2}}[A][Br_2][X]$$

When [X] = [Br_2]

$$\frac{dP}{dt} = \left(\frac{k_1k_2k_3}{k_{-1}k_{-2}}\right)[A][Br_2]^2 \quad (4)$$

When [X] = [S]

$$\frac{dP}{dt} = \left(\frac{k_1k_2k_3}{k_{-1}k_{-2}}\right)[S][A][Br_2] \quad (5)$$

where [S] = solvent. Therefore for [X] = [Br_2]

$$K_{eff} = \left(\frac{k_1k_2}{k_{-1}k_{-2}}\right)k_3$$

and the reaction is third-order. For [X] = [S]

$$K_{eff} = \left(\frac{k_1k_2[S]}{k_{-1}k_{-2}}\right)k_3$$

and the reaction is second-order.

Assuming ($k_1k_2/k_{-1}k_{-2}$) ≅ 1, on the basis of the agreement between the calculated and the experimental free energies for the reaction in a nonpolar solvent (Table 8), $K_{eff} \cong k_3$[S] for eq 5. In this case, to compare the calculated and the experimental free energies of activation, the experimental rate constant must be divided by [S]. The resulting $\Delta G^{\ddagger}_{exptl}$ is found to be 72.5 kJ mol^{-1}, which is in much better agreement with the calculated value (75.5 kJ mol^{-1} at B3LYP/BC6-31G(d)) obtained from the reaction of ethene with Br_2 mediated by a single CH_3OH molecule in CH_3OH solution (pathway G) as shown in Figure 14. This is the first evidence that a solvent molecule also takes part in the bromination reaction for polar protic solvents such as CH_3OH.

3.5. Thermodynamic Results for the Reaction of Alkenes with Br_2. The thermodynamic properties for the bromination reaction investigated are listed in Table 9. All of the reactions are found to be exothermic at all levels of theory and basis sets.

The ΔH values for the reaction of Br_2 with ethene and propene are −125.7 and −129.0 kJ mol^{-1} at G3MP2B3 and −126.0, −91.7, −123.3, −121.0, and −94.4 kJ mol^{-1} for isobutene, fluoroethene, chloroethene, (*E*)-1,2-difluoroethene, and (*E*)-1,2-dichloroethene, respectively, at G3MP2B3(BC). The enthalpies of reaction at G3MP2 and G3MP2B3 levels for the reaction of Br_2 with ethene and propene differ by no more than 1.8 kJ mol^{-1}. There is also excellent agreement between G3 theories and experimental[48] enthalpies for the reaction of Br_2 with ethene, propene, and isobutene differing by no more than 7.5 kJ mol^{-1} ($CH_3-CH_2=CH_2 + Br_2 \rightarrow$ *trans*-$CH_3-CH_2Br-CH_2Br$). However, the G3MP2B3(BC) enthalpy for (*E*)-1,2-dichloroethene differs by 22.0 kJ mol^{-1} from experiment. On the basis of the agreement between experimental and calculated enthalpies at G3 theories, the error is most likely in the experimental value. All of the reactions were also exergonic at all the levels of theory and basis sets. The free energies of reaction with ethene and propene are −84.3 and −83.8 kJ mol^{-1} at G3MP2B3 and −79.9, −43.5, −78.8, −75.6, and −47.8 kJ mol^{-1} for isobutene, fluoroethene, chloroethene, (*E*)-1,2,-difluoroethene, and (*E*)-1,2-dichloroethene, respectively at G3MP2B3(BC). In general, B3LYP provides reaction enthalpies and free energies that are in better agreement with G3 theories than HF and MP2. However, for chloroethene and (*E*)-1,2-dichloroethene, the thermodynamic values obtained using G3MP2B3(BC) fall between MP2 and B3LYP values. For the reaction with ethene, the gas-phase free energies of reaction at MP2/6-31G(d) and B3LYP/6-31G(d) levels are −110.5 and −81.3 kJ mol^{-1}, which decrease to −111.1 and −92.2 kJ mol^{-1} in CCl_4. Similarly, the MP2/6-31G(d) and B3LYP/6-31G(d) free energies for the reaction with propene are −107.1 and −68.7 kJ mol^{-1} in the gas phase, which decrease to −109.0 and −77.8 kJ mol^{-1} in CCl_4.

3.6. Performance of Theory/Basis Set. All of the reactions studied in this work are isogyric. When comparing the HF results with other levels of theory, it is evident that electron correlation is quite important in these reactions for activation energies. However, it is not that significant for reaction enthalpies and free energies. In general, activation energies calculated using MP2 consistently agree better with the G3 theories, while B3LYP appears to underestimate some activation energies. However, for pathway F, which is the likely pathway for the

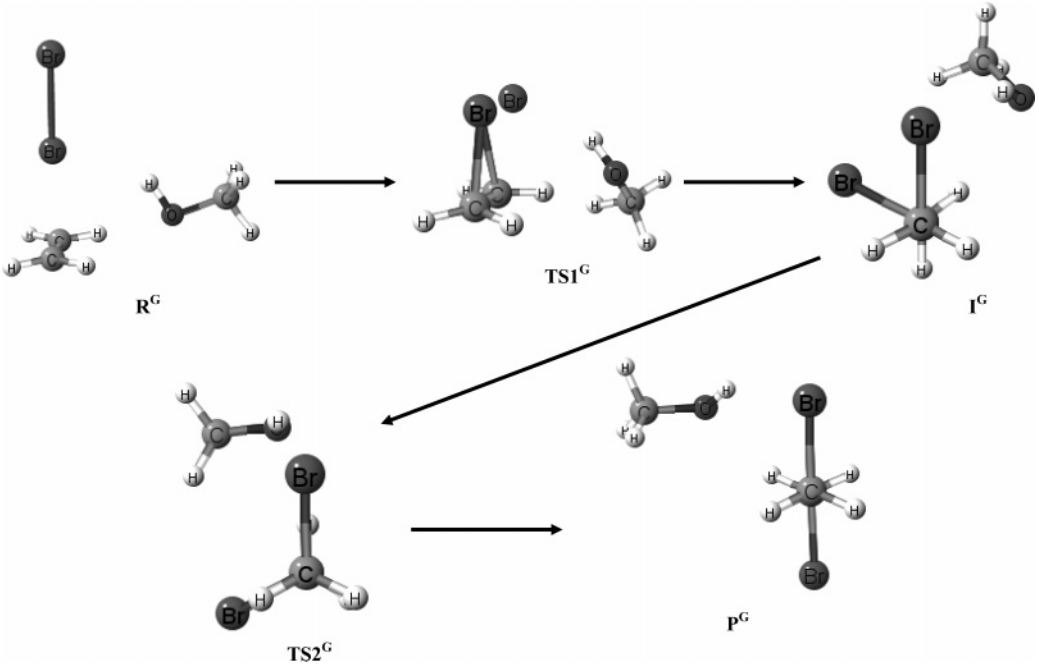

Figure 14. Mechanism for the reaction of $CH_2=CH_2 + Br_2$ mediated by a CH_3OH molecule (pathway G).

TABLE 9: Thermodynamic Properties (kJ mol^{-1}) at 298.15 K for the Reaction of $CH_2{=}CH_2$, $CH_3{-}CH_2{=}CH_2$, $(CH_3)_2CH{=}CH_2$, $CH_2{=}CHF$, $CH_2{=}CHCl$, (*E*)-$CHF{=}CHF$, and (*E*)-$CHCl{=}CHCl$ with Br_2[a]

level/basis set	ΔE	ΔG	ΔH	ΔE	ΔG	ΔH
	$CH_2{=}CH_2 + Br_2 \rightarrow CH_2Br{-}CH_2Br$			$CH_3{-}CH_2{=}CH_2 + Br_2 \rightarrow CH_3{-}CH_2Br{-}CH_2Br$		
HF/6-31G(d)	−133.2	−81.3	−121.7	−123.4	−66.5	−112.8
HF/BC6-31G(d)	−134.1	−80.8	−122.9	−130.8	−74.0	−120.4
MP2/6-31G(d)	−162.6	−110.5	−151.1	−164.2	−107.1	−153.8
CCl_4[b]		−111.1			−109.0	
MP2/BC6-31G(d)	−159.1	−106.0	−148.2	−166.3	−109.7	−156.4
B3LYP/6-31G(d)	−133.2	−81.3	−123.0	−123.5	−68.7	−114.2
CCl_4[b]		−92.2			−77.8	
B3LYP/BC6-31G(d)	−134.5	−82.8	−124.5	−131.0	−76.1	−121.8
B3LYP/6-31+G(d)	−123.1	−71.0	−112.7	−114.2	−59.2	−104.8
B3LYP/BC6−31+G(d)	−138.2	−85.1	−127.4	−147.2	−90.3	−136.9
B3P86/6-31G(d)	*d*	*d*	*d*	−147.1	−91.9	−137.6
B3P86/BC6-31G(d)	−156.9	−105.0	−146.7	−154.8	−99.8	−145.7
B3PW91/6-31G(d)	−148.3	−98.0	−138.0	−138.5	−83.3	−129.1
B3PW91/BC6-31G(d)	−149.7	−97.8	−139.5	−146.3	−91.2	−137.0
MP2/G3MP2large //MP2(FULL)/6-31G(d)	−159.6	−123.8	−163.4	−163.7	−106.3	−166.8
MP2/G3MP2large //B3LYP/6-31G(d)	−157.4	−119.8	−161.1	−160.3	−103.0	−163.2
G3MP2	−123.1	−87.3	−126.8	−127.6	−85.4	−130.8
G3MP2B3	−122.0	−84.3	−125.7	−126.0	−83.8	−129.0
experimental			−120.9 ± 1.3[c]			−122.5 ± 0.8[c]
	$(CH_3)_2C{=}CH_2 + Br_2 \rightarrow (CH_3)_2CBr{-}CH_2Br$			$CHF{=}CH_2 + Br_2 \rightarrow CHFBr{-}CH_2Br$		
HF/BC6-31G(d)	−126.1	−69.0	−116.5	−117.5	−62.7	−108.1
MP2/BC6-31G(d)	−173.7	−116.7	−164.7	−146.2	−91.5	−136.9
B3LYP/BC6-31G(d)	−125.7	−71.1	−117.5	−119.2	−66.3	−111.0
B3LYP/BC6−31+G(d)	−152.5	−95.5	−142.9	*d*	*d*	*d*
B3P86/BC6-31G(d)	−151.7	−96.8	−143.6	−139.7	−86.6	−131.4
B3PW91/ BC6-31G(d)	−141.9	−86.9	−133.7	−132.1	−78.9	−123.8
MP2/G3MP2large //B3LYP/BC6-31G(d)	−155.5	−112.0	−158.1	−138.3	−92.9	−141.1
G3MP2B3(BC)	−123.4	−79.9	−126.0	−88.9	−43.5	−91.7
experimental			−126.3[c]			
	$CHCl{=}CH_2 + Br_2 \rightarrow CHClBr{-}CH_2Br$			(*E*)-$CHF{=}CHF + Br_2 \rightarrow CHFBr{-}CHFBr$		
HF/BC6-31G(d)	−98.4	−43.5	−89.4	−117.6	−60.7	−109.2
MP2/BC6-31G(d)	−136.0	−81.1	−127.0	−151.9	−95.4	−143.8
B3LYP/6-31G(d)	−96.3	−43.1	−88.2			
B3LYP/BC6-31G(d)	−103.1	−50.0	−95.1	−121.8	−67.3	−114.8
MP2/G3MP2large //B3LYP/BC6-31G(d)	−134.6	−92.3	−137.1	−146.6	−103.6	−149.1
G3MP2B3(BC)	−120.9	−78.8	−123.3	−118.6	−75.6	−121.0
	(*E*)-$CHCl{=}CHCl + Br_2 \rightarrow CHClBr{-}CHClBr$					
HF/BC6-31G(d)	−66.4	−9.5	−59.2			
MP2/BC6-31G(d)	−117.5	−62.3	−110.3			
B3LYP/6-31G(d)	−63.7	−8.8	−57.5			
B3LYP/BC6-31G(d)	−75.4	−20.6	−69.4			
MP2/G3MP2large //B3LYP/BC6-31G(d)	−123.0	−78.6	−125.2			
G3MP2B3(BC)	−92.2	−47.8	−94.4			
experimental			−72.4[c]			

[a] The products are all in a trans conformation. [b] The PCM-UA0 model was used for optimized structures. In all cases $\Delta G = \Delta\Delta G$ (thermal correction) + ΔG_{solv}. [c] The values were obtained from ref 48. [d] Indicates missing values due to failure to optimize the transition state.

reaction of $2Br_2$ with ethene, both MP2 and B3LYP agree well with the G3 results. Activation energies calculated using the standard 6-31G(d) bromine basis set differ by no more than 16.8 kJ mol^{-1} (HF, pathway C) compared to the BC6-31G(d) basis set results, and the differences decrease from HF to MP2 and B3LYP levels of theory. There was little to no effect on the barriers by the addition of diffuse functions when compared to G3 theories. Even use of the G3MP2large basis set does not improve the barriers.

For thermodynamics, the G3MP2 and G3MP2B3 theories differ by no more than 3 kJ mol^{-1} for reaction enthalpies and free energies (ΔG for $CH_2{=}CH_2 + Br_2 \rightarrow CH_2Br{-}CH_2Br$). The G3 theories are also in excellent agreement with experiment, except in the case of $CHCl{=}CHCl + Br_2 \rightarrow CHClBr{-}CHClBr$, where B3LYP/BC6-31G(d) differs by only 3 kJ mol^{-1}, where as G3MP2B3(BC) differs by 22 kJ mol^{-1} from experiment.[48] In comparison to MP2, thermodynamic values calculated using B3LYP provide reaction enthalpies and free energies that are consistently in better agreement with G3 values. Thermodynamic values calculated using the standard 6-31G(d) bromine basis set differ by no more than 8.1 kJ mol^{-1} (B3P86, $CH_3{-}CH_2{=}H_2 + Br_2 \rightarrow CH_3{-}CH_2Br{-}CH_2Br$) compared to the Binning−Curtiss 6-31G(d) basis set results. However, the reaction enthalpies and free energies differ significantly when diffuse functions are added to the two basis sets. For example, the enthalpy for $CH_3{-}CH_2{=}CH_2 + Br_2 \rightarrow CH_3{-}CH_2Br{-}CH_2Br$ calculated at the B3LYP/6-31+G(d) and B3LYP/BC6−31+G(d) levels of theory differs by 32.1 kJ mol^{-1}.

3.7. Exploring Heats of Formation (ΔH_f). From the ΔH values of reactions calculated at the G3 theories in this study, it is possible to calculate heats of formation for some alkenes

TABLE 10: Heats of Formation, ΔH_f, (kJ mol^{-1}) at 298.15 K[a]

species	ΔH_f experimental[b]	ΔH_f present work	species	ΔH_f experimental	ΔH_f present work
CH_2=CH_2	52.57	57.3	*trans*-CHFBr−CH_2Br		−214.8
trans-CH_2Br−CH_2Br	−37.52	−42.3	CH_2=CHCl	29.0[b]	
CH_3−CH_2=CH_2	20.41	26.9	*trans*-CHClBr−CH_2Br		−63.4
trans-CH_3−CH_2Br−CH_2Br	−71.18	−77.7	(*E*)-CHF=CHF	−310.0[c]	
$(CH_3)_2$CH=CH_2	−17.9 ± 1.1	−18.2	*trans*-CHFBr−CHFBr		−400.1
trans-$(CH_3)_2$CBr−CH_2Br	−113.3 ± 1.0	−113.0	(*E*)-CHCl=CHCl	1.7[b]	
Br_2	30.91		*trans*-CHClBr−CHClBr		−61.8
CH_2=CHF	−136.0				

[a] See text for explanation. [b] Reference 48 [c] Reference 49.

and dibromoalkanes. The ΔH_f values obtained in this study are given in Table 10.

From the G3MP2B3 enthalpy of reaction for CH_2=CH_2 + Br_2 → *trans*-CH_2Br−CH_2Br (−125.7 kJ mol^{-1}) and the most recent and reliable experimental ΔH_f(CH_2=CH_2) and ΔH_f(Br_2) (given in Table 10), ΔH_f(*trans*-CH_2Br−CH_2Br) is calculated to be −42.3 kJ mol^{-1}, which is in good agreement with experiment (−37.52 kJ mol^{-1}). Similarly, ΔH_f(CH_2=CH_2) is calculated from the same reaction enthalpy and by using the experimental ΔH_f(Br_2) and ΔH_f(*trans*-CH_2Br−CH_2Br). The resulting ΔH_f(CH_2=CH_2) is 57.3 kJ mol^{-1}, the value being in excellent agreement with experiment. Following the same procedure, it was possible to calculate ΔH_f for CH_3−CH_2=CH_2, *trans*-CH_3−CH_2Br−CH_2Br, $(CH_3)_2$C=CH_2, and *trans*-$(CH_3)_2$CBr−CH_2Br using the enthalpies of reaction for CH_3−CH_2=CH_2 + Br_2 → *trans*-CH_3−CH_2Br−CH_2Br (−129.0 kJ mol^{-1} at G3MP2B3) and $(CH_3)_2$C=CH_2 + Br_2 → *trans*-$(CH_3)_2$-CBr−CH_2Br (−126.0 kJ mol^{-1} at G3MP2B3(BC)), along with experimental ΔH_f values for Br_2, CH_3−CH_2=CH_2, *trans*-CH_3−CH_2Br−CH_2Br, $(CH_3)_2$C=CH_2, and *trans*-$(CH_3)_2$CBr−CH_2Br obtained from the literature. These ΔH_f values are also in excellent agreement with the experimental values, all within 6.6 kJ mol^{-1}. No experimental or theoretical ΔH_f values have been reported for *trans*-CHFBr−CH_2Br, *trans*-CHClBr−CH_2-Br, (*E*)-CHFBr=CHFBr, and (*E*)-CHClBr=CHClBr. In this study, ΔH for CHF=CH_2 + Br_2 → *trans*-CHFBr−CH_2Br (−91.7 kJ mol^{-1} at G3MP2B3(BC)), CHCl=CH_2 + Br_2 → *trans*-CHClBr−CH_2Br (−123.3 kJ mol^{-1} at G3MP2B3(BC)), (*E*)-CHF=CHF + Br_2 → *trans*-CHFBr−CHFBr (−121.0 kJ mol^{-1} at G3MP2B3(BC)), and (*E*)-CHCl=HCl + Br_2 → *trans*-CHClBr−CHClBr (−94.4 kJ mol^{-1} at G3MP2B3(BC)) have been obtained. From this data and the experimental ΔH_f values of CHF=H_2, CHCl=H_2, (*E*)-CHF=HF, and (*E*)-CHCl=HCl, the ΔH_f values for *trans*-CHFBr−CH_2Br, *trans*-CHClBr−CH_2-Br, *trans*-CHFBr−CHFBr, and *trans*-CHClBr−CHClBr were calculated to be −214.8, −63.4, −400.1, and −61.8 kJ mol^{-1}, respectively.

4. Conclusions

A comprehensive investigation was conducted on the possible mechanisms involved in the reaction of alkenes with Br_2 and $2Br_2$. It has been found that there are two possible mechanisms for the reaction of alkenes with one Br_2, one involving a perpendicular attack on the C=C double bond producing a bromonium/Br^- ion pair. However, the mechanism does not lead to product. The other pathway is a sidewise attack by a Br_2 on the C=C bond, producing first a bromonium/Br^- ion pair followed by formation of the *trans*-1,2-dibromoalkane. Therefore, the only mechanism found for reaction with one Br_2 molecule producing *trans*-1,2-dibromoalkane is through sidewise attack by Br_2. Reaction of ethene with $2Br_2$ involves several different pathways all producing *trans*-1,2-dibromoalkane as the product. The overall reaction barrier is the lowest for the reaction of ethene + $2Br_2$. The bromination reactions of alkenes in CCl_4 predict mechanisms similar to that obtained in the gas phase. However, the solvent model predicts a lowering of free energies of activation for the rate-determining steps of all of the reactions in CCl_4 solution. The overall free energy of activation obtained from the most likely pathway (pathway F) involving $2Br_2$ is in excellent agreement with experiment for the reaction in nonpolar aprotic solvents. For polar protic solvents, the calculated activation energies obtained from the reaction with a single Br_2 mediated by a solvent molecule are in excellent agreement with experiment. The calculated free energies of activation decrease with the polarity of solvents, which is in agreement with the experimental observations (Table 8). All of the reactions are found to be exothermic and exergonic for the formation of the *trans*-1,2-dibromoalkane product.

Acknowledgment. We thank Dr. Travis Fridgen for his valuable advice and suggestions. We are also grateful to the Natural Sciences and Engineering Council of Canada for financial support and the Atlantic Computational Excellence Network for computer time.

Supporting Information Available: Full geometries and energies of all structures for the reaction of alkene with Br_2 and $2Br_2$. This material is available free of charge via the Internet at http://pubs.acs.org.

References and Notes

(1) Smith, M. B.; March, J. *March's Advanced Organic Chemistry: Reactions, Mechanisms, and Structure*, 6th ed.; Wiley-Interscience: Hoboken, NJ, 2007.

(2) de la Mare, P. B. D.; Bolton, R. *Electrophilic Additions to Unsaturated Systems*, 2nd ed.; Elsevier: New York, 1982.

(3) Brown, R. S.; Slebocka-Tilk, H.; Bennet, A. J.; Bellucci, G.; Bianchini, R.; Ambrosetti, R. *J. Am. Chem. Soc.* **1990**, *112*, 6310−6316.

(4) Schmid, G. H.; Garrat, D. G. In *The Chemistry of Double-Bonded Functional Groups*; Patai, S., Ed.; Wiley: New York, 1977; Suppl. A, Part 2, p 725.

(5) Brown, R. S.; Gedye, R.; Slebocka-Tilk, H.; Buschek, J.; Kopecky, K. *J. Am. Chem. Soc.* **1984**, *106*, 4515−4521.

(6) Bellucci, G.; Chiappe, C.; Marioni, F. *J. Am. Chem. Soc.* **1987**, *109*, 515−522.

(7) Bellucci, G.; Bianchini, R.; Chiappe, C.; Marioni, F.; Spagna, R. *J. Am. Chem. Soc.* **1988**, *110*, 546−552.

(8) Roberts, I.; Kimball, G. E. *J. Am. Chem. Soc.* **1937**, *59*, 947.

(9) Olah, G. A.; Bollinger, J. M. *J. Am. Chem. Soc.* **1968**, *90*, 947.

(10) Olah, G. A.; Bollinger, J. M.; Brinich, J. *J. Am. Chem. Soc.* **1968**, *90*, 2587.

(11) Berman, D. W.; Anicich, V.; Beauchamp, J. L. *J. Am. Chem. Soc.* **1979**, *101*, 1239−1248.

(12) Wieting, R. D.; Staley, R. H.; Beauchamp, J. L. *J. Am. Chem. Soc.* **1974**, *96*, 7552−7554.

(13) Staley, R. H.; Wieting, R. D.; Beauchamp, J. L. *J. Am. Chem. Soc.* **1977**, *99*, 5964−5972.

(14) Kim, J. K.; Findlay, M. C.; Henderson, W. G.; Caserio, M. C. *J. Am. Chem. Soc.* **1973**, *95*, 2184−2193.
(15) Angelini G.; Speranza M. *J. Am. Chem. Soc.* **1981**, *103*, 3792−3799.
(16) Tsai, B. P.; Werner, A. S.; Baer, T. *J. Chem. Phys.* **1975**, *63*, 4384−4392.
(17) McLafferty, F. W. *Anal. Chem.* **1962**, *34*, 2−15.
(18) Strating, J.; Wieringa, J. H.; Wynberg, H. *J. Chem. Soc. D* **1969**, 907−908.
(19) Slebocka-Tilk, H.; Ball, R. G.; Brown, R. S. *J. Am. Chem. Soc.* **1985**, *107*, 4504−4508.
(20) Bellucci, G.; Chiappe, C.; Bianchini, R.; Lenoir, D.; Herges, R. *J. Am. Chem. Soc.* **1995**, *117*, 12001−12002.
(21) Olah, G. A.; Prakash, G. K. S. *J. Org. Chem.* **1977**, *42*, 580.
(22) Koerner, T.; Brown, R. S.; Gainsforth J. L.; Klobukowski, M. *J. Am. Chem. Soc.* **1998**, *120*, 5628−5636.
(23) Chretien, J. R.; Coudert, J.; Ruasse, M. *J. Org. Chem.* **1993**, *58*, 1917−1921.
(24) Olah, G. A. *Halonium Ions*; Wiley: New York, 1975.
(25) Garnier, F.; Dubois, J. E. *Bull. Soc. Chim. Fr.* **1968**, 3797.
(26) Olah, G. A.; Hockswender, T. R., Jr. *J. Am. Chem. Soc.* **1974**, *96*, 3574.
(27) Yamabe, S.; Minato, T.; Inagaki, S. *J. Chem. Soc., Chem. Commun.* **1988**, 532.
(28) Hamilton, T. P.; Schaefer, H. F. *J. Am. Chem. Soc.* **1990**, *112*, 8260−8265.
(29) Cammi, R.; Mennucci, B.; Pomelli, C.; Cappelli, C.; Corni, S.; Frediani, L.; Trucks, G. W.; Frisch, M. J. *Theor. Chem. Acc.* **2004**, *111*, 66−77.
(30) Strnad, M.; Martins-Costa, M. T. C.; Millot, C.; Tunon, I.; Ruiz-Lopez, M. F.; Rivail, J. L. *J. Chem. Phys.* **1997**, *106*, 3643−57.
(31) Hamilton, T. P.; Schaefer, H. F. *J. Am. Chem. Soc.* **1991**, *113*, 7147−7151.
(32) Cossi, M.; Persico, M.; Tomas, J. *J. Am. Chem. Soc.* **1994**, *116*, 5373−5378.
(33) Chiappe, C.; Lenoir, D.; Pomelli, C. S.; Bianchini, R. *Phys. Chem. Chem. Phys.* **2004**, *6*, 3235−3240.
(34) Ruiz, E.; Salahub, D. R.; Vela, A. *J. Am. Chem. Soc.* **1995**, *117*, 1141−1142.
(35) Lenoir, D.; Chiappe, C. *Chem.—Eur. J.* **2003**, *9*, 1036−1044.
(36) Curtiss, L. A.; Redfern, P. C.; Raghavachari, K.; Rassolov, V.; Pople, J. A. *J. Chem. Phys.* **1999**, *110*, 4703.
(37) Baboul, A. G.; Curtiss, L. A.; Redfern, P. C.; Raghavachari, K. *J. Chem. Phys.* **1999**, *110*, 7650.
(38) Frisch, M. J.; Trucks, G. W.; Schlegel, H. B.; Scuseria, G. E.; Robb, M. A.; Cheeseman, J. R.; Montgomery, J. A., Jr.; Vreven, T.; Kudin, K. N.; Burant, J. C.; Millam, J. M.; Iyengar, S. S.; Tomasi, J.; Barone, V.; Mennucci, B.; Cossi, M.; Scalmani, G.; Rega, N.; Petersson, G. A.; Nakatsuji, H.; Hada, M.; Ehara, M.; Toyota, K.; Fukuda, R.; Hasegawa, J.; Ishida, M.; Nakajima, T.; Honda, Y.; Kitao, O.; Nakai, H.; Klene, M.; Li, X.; Knox, J. E.; Hratchian, H. P.; Cross, J. B.; Bakken, V.; Adamo, C.; Jaramillo, J.; Gomperts, R.; Stratmann, R. E.; Yazyev, O.; Austin, A. J.; Cammi, R.; Pomelli, C.; Ochterski, J. W.; Ayala, P. Y.; Morokuma, K.; Voth, G. A.; Salvador, P.; Dannenberg, J. J.; Zakrzewski, V. G.; Dapprich, S.; Daniels, A. D.; Strain, M. C.; Farkas, O.; Malick, D. K.; Rabuck, A. D.; Raghavachari, K.; Foresman, J. B.; Ortiz, J. V.; Cui, Q.; Baboul, A. G.; Clifford, S.; Cioslowski, J.; Stefanov, B. B.; Liu, G.; Liashenko, A.; Piskorz, P.; Komaromi, I.; Martin, R. L.; Fox, D. J.; Keith, T.; Al-Laham, M. A.; Peng, C. Y.; Nanayakkara, A.; Challacombe, M.; Gill, P. M. W.; Johnson, B.; Chen, W.; Wong, M. W.; Gonzalez, C.; Pople, J. A. *Gaussian 03*, revision B.05; Gaussian, Inc.: Wallingford, CT, 2004.
(39) Islam, S. M.; Hollett, J. W.; Poirier, R. A. *J. Phys. Chem. A* **2007**, *111*, 526−540.
(40) Rassolov, V. A.; Ratner, M. A.; Pople, J. A.; Redfern, P. C.; Curtiss, L. A. *J. Comput. Chem.* **2001**, *22*, 976−984.
(41) Binning, R. C., Jr.; Curtiss, L. A. *J. Comput. Chem.* **1990**, *11*, 1206.
(42) Curtiss, L. A.; Redfern, P. C.; Rassolov, V.; Kedziora, G. S.; Pople, J. A. *J. Chem. Phys.* **2001**, *114*, 9287.
(43) Curtiss, L. Computational Thermochemistry. http://chemistry.anl.gov/compmat/comptherm.htm (accessed July 15, 2007).
(44) Dubois, J. E.; Mouvier, G. *Tetrahedron Lett.* **1963**, 1325.
(45) Dubois, J. E.; Mouvier, G. *Bull. Soc. Chim. Fr.* **1968**, 1426.
(46) Modro, A.; Schmid, G. H.; Yates, K. *J. Org. Chem.* **1977**, *42*, 3673−3676.
(47) Hanna, J. G.; Siggia, S. *Anal. Chem.* **1965**, *37*, 690.
(48) Chase, M. W. NIST-JANAF Thermochemical Tables, 4th ed. *J. Phys. Chem. Ref. Data* **1998**, (Monograph 9), 1−1951.
(49) Wagman, D. D.; Evans, W. H.; Parker, V. B.; Shumm, R. H.; Halow, I.; Bailey, S.M.; Churney, K. L.; Nuttall, R. L. *J. Phys. Chem. Ref. Data.* **1982**, *11* (2).